doi.org/10.26434/chemrxiv.12901304.v1

Organocatalyzed Fluoride Metathesis

Mark Crimmin, Daniel Mulryan, Andrew J. P. White

Submitted date: 01/09/2020 • Posted date: 01/09/2020

Citation information: Crimmin, Mark; Mulryan, Daniel; White, Andrew J. P. (2020): Organocatalyzed Fluoride Metathesis. ChemRxiv. Preprint. https://doi.org/10.26434/chemrxiv.12901304.v1

A new organocatalyzed fluoride metathesis reaction between fluoroarenes and carbonyl derivatives is reported. The reaction exchanges fluoride (F−) and alternate nucleophiles (OAc−, CO2R−, SR−, Cl−, CN−, NCS−). The approach provides a conceptually novel route to manipulate the fluorine content of organic molecules. By combining fluorination and defluorination steps into a single catalytic cycle, a byproduct free and 100% atom-efficient reaction can be achieved.

Organocatalyzed Fluoride Metathesis

Daniel Mulryan, Andrew J. P. White and Mark R. Crimmin*

Department of Chemistry, Molecular Sciences Research Hub, Imperial College London, White City, Shepherds Bush, W12 0BZ, UK

Abstract: A new organocatalyzed fluoride metathesis reaction between fluoroarenes and carbonyl derivatives is reported. The reaction exchanges fluoride (F^-) and alternate nucleophiles (OAc^-, CO_2R^-, SR^-, Cl^-, CN^-, NCS^-). The approach provides a conceptually novel route to manipulate the fluorine content of organic molecules. By combining fluorination and defluorination steps into a single catalytic cycle, a byproduct free and 100% atom-efficient reaction can be achieved.

Fluorine is ubiquitous in organic synthesis. From modulating the bioavailability of agrochemicals and pharmaceuticals, to improving the chemical stability of refrigerants and polymers, fluorine plays a key role in chemical manufacturing.[1-4] Despite their importance, our current approach to the synthesis of fluorochemicals is not sustainable. Inorganic fluoride (fluorspar, CaF_2) is converted into HF which is ultimately used as the fluorine source for nearly all synthetic organofluorine compounds. Current estimates suggest that viable sources of fluorspar will sustain the fluorocarbons industry for less than 100 years.[5] Others have begun to question the long-term strategy behind the use of this finite resource.[6] Fluorine containing molecules are often treated as single use and can result in environmental contamination, leading to significant issues such as ozone depletion, global warming, and water contamination. Further to these concerns our current approaches to install and remove fluorine atoms into organic molecules are wasteful. Fluorination reagents such as tetrabutylammonium fluoride (TBAF), diethylaminosulfur trifluoride (DAST), and 1-chloromethyl-4-fluoro-1,4-diazonoabicyclo[2.2.2]octane bis(tetrafluoroborate) (selectfluor®), have low atom-efficiency, while defluorination methods often rely on stoichiometric main group reagents such as silanes or boranes to provide a thermodynamic driving force for breaking strong carbon–fluorine bonds.[7-9]

In this paper we describe an alternative approach to manipulate the fluorine content of molecules. We report an organocatalyzed fluoride metathesis reaction which involves the exchange of F^- with a wide variety of functional groups including acetate, carboxylate, thiol, chloride, cyanide and isothiocyanate (eq. 1). The reaction transfers the fluoride group between organic fragments.

$$R^1{-}F + R^2{-}X \rightleftharpoons R^1{-}X + R^2{-}F \quad \text{(eq. 1)}$$

Very recently Saunders and co-workers reported a stoichiometric fluoride metathesis reaction promoted by a Rh complex[10] The finding builds upon the pioneering work of Yamaguchi and co-workers who used $[RhH(PPh_3)_3]$ to establish exchange equilibria between fluoroarenes and esters or thioesters to form functionalised arenes and carbonyl fluorides.[11,12] These papers suggest a general approach to catalytic fluoride metathesis should be viable, but the current systems are constrained to stoichiometric or expensive metals and are limited in scope.

We became interested in the idea of using simple nucleophilic catalysts to achieve fluoride metathesis. In 2005, Sandford and co-workers reported the S_NAr reaction of 4-dimethylaminopyridine (DMAP) and pentafluoropyridine to form a pyridinium fluoride salt (Figure 1a).[13] This salt could be isolated and used as a nucleophilic source of F^- for the fluorination of a limited scope of organohalides. The studies form part of a broader set of work which targets the generation of anhydrous F^- by the combination of two organic components.[14-18] Interestingly, Schmidt and co-workers reported that the same pyridinium fluoride salt served as an electrophile in reactions with external nucleophiles.[19] We envisaged that these two modes of reactivity could be combined to create a catalytic method for fluoride metathesis (Figure 1b).

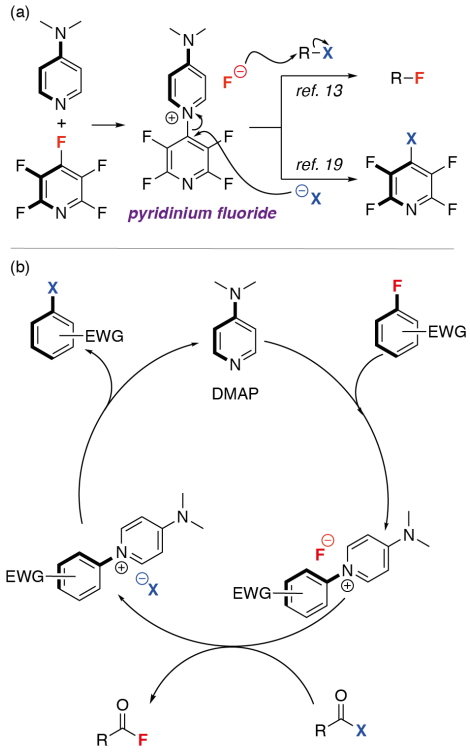

Figure 1. (a) A pyridinium salt from S_NAr addition of DMAP to pentafluoropyridine and its established reactivity. (b) A proposed catalytic cycle for fluoride metathesis.

In a series of experiments, we established the metathesis reaction between pefluoroarenes and suitable partners (acid anhydrides, dimethyl dicarbonate, s-phenyl thioacetate, benzoyl chloride, benzoyl cyanide, benzoyl isothiocyanate). Reactions were conducted with pentafluoropyridine as the fluoroarene of choice, due to it being activated towards reactions with nucleophiles by S_NAr. Following an initial screening of conditions and substrates, a reaction scope was developed in which pentafluoropyridine was reacted with a series of functional groups in the presence of 5 mol% DMAP catalyst in acetonitrile at 100 °C. The fluoride metathesis reaction creates two products, a new functionalisation fluoroarene (**1a-q**) and an acyl fluoride (**2a-e**), both of which contain usable fluorine content. Formation of the acyl fluoride provides a thermodynamic driving force for the forward reaction. In all cases, yields were recorded for both fluoride metathesis products and there is a clear and expected correlation between the yields of **1** and **2**. The reaction scope includes a variety of metathesis partners meaning it can be used as a general approach to create C–O, C–Cl, C–C, C–N and C–S bonds from high fluorine content arenes (Table 1).

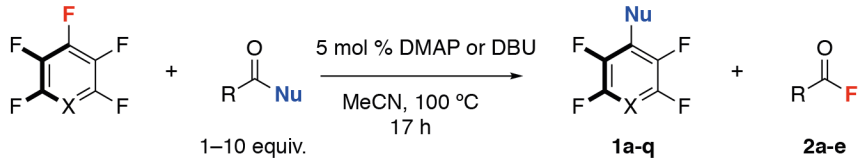

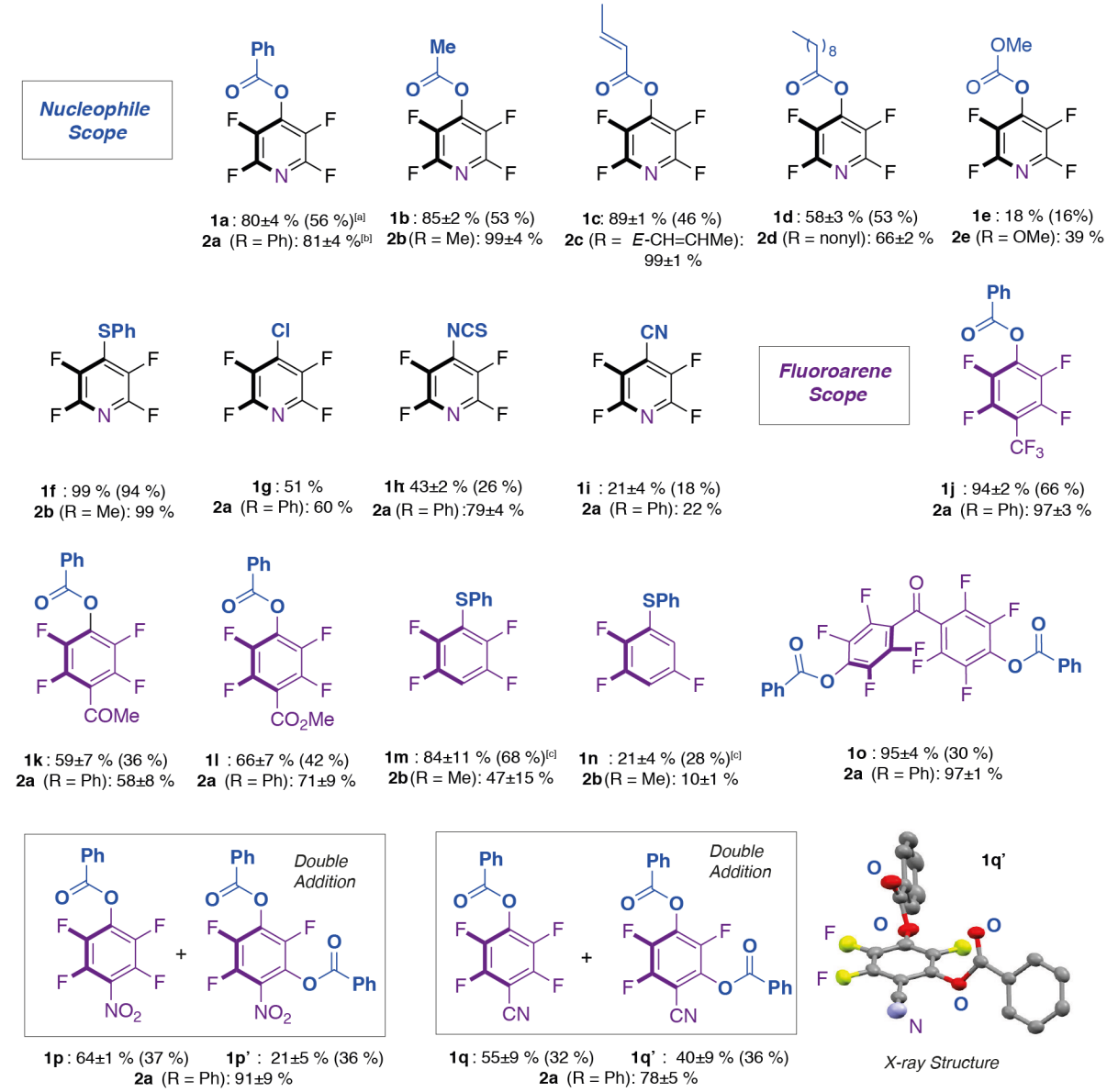

Table 1. Fluoride metathesis reaction of fluoroarenes with a range of different carbonyl derived functional groups. [a] Internal NMR yield of tetr fluoropyridine product using ^{19}F NMR (isolated yield after workup in parenthesis). [b] Internal NMR yield of the corresponding carbonyl fluoride using ^{19}F NMR. Standard deviation calculated from three repeats at a 99.9% confidence. [c] DBU was used as a catalyst.

The observed regioselectivity is consistent with that expected from a concerted or stepwise S_NAr mechanism. Yields of the reaction decreased for less stable nucleophiles such as carboxylates (prone to eliminate CO_2) and lower fluorine content arenes. For the highly reactive substrates pentafluorobenzonitrile and pentafluoronitrobenzene, a mixture of mono and disubstituted products were observed. In most cases, the disubstituted species was the minor product. Use of *S*-phenyl thioacetate to generate the highly nucleophilic benzenethiolate anion enabled expansion of the scope and fluoride metathesis of the less activated fluoroarenes pentafluorobenzene and 1,2,3,5-tetrafluorobenzene (**1m** and **1n**, Table 1). Interestingly, these reactions required the presence of 5 mol % of DBU to proceed and no conversion was observed when DMAP was used as a catalyst.[20] DBU proved a poorer catalyst for other reactions in the series and no product was observed for fluoride metathesis of pentafluorobenzene with benzoic anhydride using this catalyst.

Both the reaction products of fluoride metathesis are useful chemical intermediates. Substituted polyfluoroarenes are featured in liquid-crystal displays[21,22] and conjugated polymers for organic light-emitting diodes.[23,24] They are also useful building blocks for the synthesis of partially fluorinated arenes relevant to drug discovery through a further hydrodefluorination step.[25-27] Acyl fluorides are versatile fluorinating agents for a variety of reactions including: oxidative addition to transition metals;[27,28] the enantioselective ring-opening fluorination of epoxides,[29] and the hydrofluorination of alkynes.[30]

A series of experiments and calculations were undertaken to interrogate the proposed mechanism of fluoride metathesis. Monitoring the reaction of pentafluoropyridine with benzoic anhydride catalyzed by 5 mol % DMAP by ^{19}F NMR spectroscopy shows that **1a** and **2a** are formed at the same rate (supporting information). In further experiments, the direct reaction of DMAP with both pentafluoropyridine and acetyl anhydride could be observed. Hence, the stoichiometric reaction of DMAP with pentafluoropyridine forms the salt **3** through nucleophilic displacement of a fluoride group from the arene. Experimentally, this salt was found to be catalytically competent for the fluoride metathesis of pentafluoropyridine and benzoic anhydride to form **1a** and **2a**. Similarly, the stoichiometric reaction of DMAP with benzoic anhydride forms the salt **4** which was again catalytically competent (Figure 2a).

Kinetic analysis reveals the reaction to be 1st order in fluoroarene, 1st order in acid anhydride, and 2nd order in DMAP. These findings were verified by both initial rates and graphical analysis (VTNA, supporting info). The second order behaviour of catalyst in the empirical rate-law is notable as it implies a turnover-limiting sequence involving two equiv. of DMAP. The most sensible interpretation of this finding is that the catalyst plays a dual role in activating *both* components of the fluoride metathesis reaction and turnover occurs by two intersecting catalytic cycles each of which relies on DMAP as a catalyst (Figure 2b).

DFT calculations were undertaken to gain a greater appreciation of the key steps involved in substrate activation in each of these intersecting cycles. The B3LYP functional and a hybrid basis set were employed. Solvent (MeCN) and dispersion corrections were considered during the optimisation of stationary points. This computational approach has been used previously to model acetylisation reactions catalysed by DMAP.[31,32]

The overall reaction of pentafluoropyridine and acetic anhydride is calculated to be exergonic by –5.8 kcal mol^{-1}. The key steps of two intersecting catalytic cycles were calculated. One involving the activation of the anhydride by DMAP and the other the activation of the fluoroarene by DMAP. The transition states associated with both intersecting pathways occur by either a concerted S_NAr or a concerted nucleophilic addition-elimination step. Catalyst activation of *both* substrates is calculated to be facile under the reaction conditions. Hence reaction of DMAP with both pentafluoropyridine (**TS-1**, $\Delta G^{\ddagger}$ = 18.0 kcal mol^{-1}) and acetic anhydride (**TS-2**, $\Delta G^{\ddagger}$ = 14.1 kcal mol^{-1}) occur by low energy barriers. The calculations also show that DMAP activated substrates are more susceptible to nucleophilic attack by F^- or OAc^- than the parent reagents (supporting information).

Based on the analysis, the turnover limiting step is predicted to be associated with **TS-3** and the nucleophilic attack of the liberated fluoride anion on the acetylated DMAP fragment of **Int-2**. While the complexity of modelling explicit solvation in this system means that this conclusion should be treated with care, if this step is turnover limiting it would be consistent with the empirical rate law and 2nd order dependence on the catalyst.

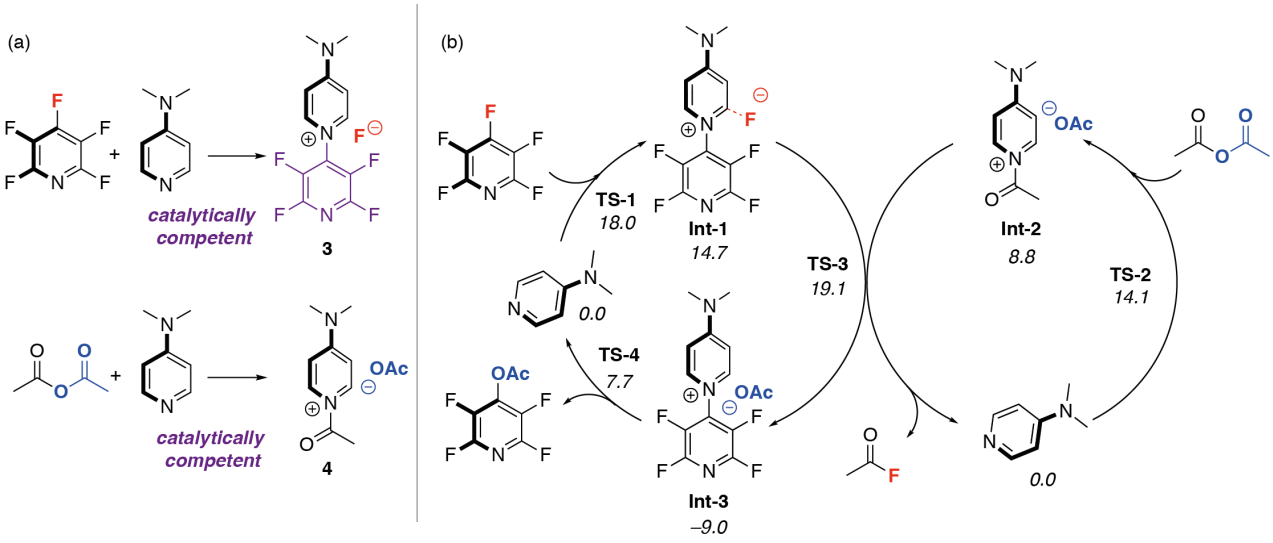

Figure 2. (a) Generation and catalytic competence of proposed intermediates **3** and **4**. (b) Proposed reaction pathway for the reaction of DMAP, C_5F_4N and acetic anhydride.

In summary, we have developed the first organocatalysed fluoride metathesis reaction. This approach is complementary to more established and less efficient methods for the fluorination and defluorination of organic molecules. By combining the two steps in a single catalytic cycle a conceptually new approach to manipulating the fluorine content of organic molecules has been achieved. This approach is 100 % atom-efficient and avoids the use of highly acidic or toxic fluorinating agents. While the reaction is currently limited to activated fluoroarenes, in the longer term the development more active catalysts or alternative strategies, such as π-activation of the arene, may allow fluoride metathesis to be established as a broad approach in the sustainable chemistry of fluorocarbons.

ASSOCIATED CONTENT

The Supporting Information is available free of charge on the ACS Publications website. X-ray crystallographic data for **1k** and **1q'** are available from the Cambridge Crystallographic Data Centre (CCDC 2021812-2021813) and as a .cif file, full details of the experiments and calculations are available as a .pdf.

Corresponding Author

*m.crimmin@imperial.ac.uk

Funding Sources

No competing financial interests have been declared. We are grateful to the ERC (FluoroFix: 677367) for generous funding.

REFERENCES

(1) Inoue, M.; Sumii, Y.; Shibata, N. Contribution of Organofluorine Compounds to Pharmaceuticals. *ACS Omega* **2020**, *5*, 10633-10640.
(2) Johnson, B. M.; Shu, Y.-Z.; Zhuo, X.; Meanwell, N. A. Metabolic and Pharmaceutical Aspects of Fluorinated Compounds. *J. Med. Chem.* **2020**, *63*, 6315-6386.
(3) Meanwell, N. A. Fluorine and Fluorinated Motifs in the Design and Application of Bioisosteres for Drug Design. *J. Med. Chem.* **2018**, *61*, 5822-5880.
(4) O'Hagan, D. Understanding organofluorine chemistry. An introduction to the C–F bond. *Chem. Soc. Rev.* **2008**, *37*, 308-319.
(5) Harsanyi, A.; Sandford, G. Organofluorine chemistry: applications, sources and sustainability. *Green Chem.* **2015**, *17*, 2081-2086.
(6) Caron, S. Where Does the Fluorine Come From? A Review on the Challenges Associated with the Synthesis of Organofluorine Compounds. *Org. Process Res. Dev.* **2020**, *24*, 470-480.
(7) Teltewskoi, M.; Panetier, J. A.; Macgregor, S. A.; Braun, T. A Highly Reactive Rhodium(I)–Boryl Complex as a Useful Tool for C-H Bond Activation and Catalytic C–F Bond Borylation. *Angew. Chem., Int. Ed.* **2010**, *49*, 3947-3951.
(8) Zámostná, L.; Ahrens, M.; Braun, T. Catalytic hydrodefluorination of fluoroaromatics with silanes as hydrogen source at a binuclear rhodium complex: Characterization of key intermediates. *J. Fluor. Chem.* **2013**, *155*, 132-142.
(9) Senaweera, S.; Weaver, J. D. S_NAr catalysis enhanced by an aromatic donor–acceptor interaction; facile access to chlorinated polyfluoroarenes. *Chem. Commun.* **2017**, *53*, 7545-7548.
(10) Morgan, P. J.; Hanson-Heine, M. W. D.; Thomas, H. P.; Saunders, G. C.; Marr, A. C.; Licence, P. C–F Bond Activation of a Perfluorinated Ligand Leading to Nucleophilic Fluorination of an Organic Electrophile. *Organometallics* **2020**, *39*, 2116-2124.
(11) Arisawa, M.; Yamada, T.; Yamaguchi, M. Rhodium-catalyzed interconversion between acid fluorides and thioesters controlled using heteroatom acceptors. *Tetrahedron Lett.* **2010**, *51*, 6090-6092.
(12) Arisawa, M.; Igarashi, Y.; Kobayashi, H.; Yamada, T.; Bando, K.; Ichikawa, T.; Yamaguchi, M. Equilibrium shift in the rhodium-catalyzed acyl transfer reactions. *Tetrahedron* **2011**, *67*, 7846-7859.
(13) Murray, C. B.; Sandford, G.; Korn, S. R.; Yufit, D. S.; Howard, J. A. K. New fluoride ion reagent from pentafluoropyridine. *J. Fluor. Chem.* **2005**, *126*, 569-574.
(14) Sun, H.; DiMagno, S. G. Anhydrous Tetrabutylammonium Fluoride. *J. Am. Chem. Soc.* **2005**, *127*, 2050-2051.
(15) Sun, H.; DiMagno, S. G. Room-Temperature Nucleophilic Aromatic Fluorination: Experimental and Theoretical Studies. *Angew. Chem., Int. Ed.* **2006**, *45*, 2720-2725.
(16) Allen, L. J.; Muhuhi, J. M.; Bland, D. C.; Merzel, R.; Sanford, M. S. Mild Fluorination of Chloropyridines with in Situ Generated Anhydrous Tetrabutylammonium Fluoride. *J. Org. Chem.* **2014**, *79*, 5827-5833.
(17) Ryan, S. J.; Schimler, S. D.; Bland, D. C.; Sanford, M. S. Acyl Azolium Fluorides for Room Temperature Nucleophilic Aromatic Fluorination of Chloro- and Nitroarenes. *Org. Lett.* **2015**, *17*, 1866-1869.
(18) Cismesia, M. A.; Ryan, S. J.; Bland, D. C.; Sanford, M. S. Multiple Approaches to the In Situ Generation of Anhydrous Tetraalkylammonium Fluoride Salts for S_NAr Fluorination Reactions. *J. Org. Chem.* **2017**, *82*, 5020-5026.
(19) Schmidt, A.; Mordhorst, T.; Namyslo, J. C.; Telle, W. Hetarenium salts from pentafluoropyridine. Syntheses, spectroscopic properties, and applications. *J. Heterocycl. Chem.* **2007**, *44*, 679-684.
(20) Baidya, M.; Mayr, H. Nucleophilicities and carbon basicities of DBU and DBN. *Chem. Commun.* **2008**, 1792-1794.
(21) Kirsch, P. Fluorine in liquid crystal design for display applications. *J. Fluor. Chem.* **2015**, *177*, 29-36.
(22) Kirsch, P.; Bremer, M. Nematic Liquid Crystals for Active Matrix Displays: Molecular Design and Synthesis. *Angew. Chem., Int. Ed.* **2000**, *39*, 4216-4235.
(23) Kamata, T.; Sasabe, H.; Watanabe, Y.; Yokoyama, D.; Katagiri, H.; Kido, J. A series of fluorinated phenylpyridine-based electron-transporters for blue phosphorescent OLEDs. *J. Mater. Chem. C* **2016**, *4*, 1104-1110.
(24) Ragni, R.; Punzi, A.; Babudri, F.; Farinola, G. M. Organic and Organometallic Fluorinated Materials for Electronics and Optoelectronics: A Survey on Recent Research. *Eur. J. Inorg. Chem.* **2018**, *2018*, 3500-3519.
(25) Dolbier, W. R. Fluorine chemistry at the millennium. *J. Fluor. Chem.* **2005**, *126*, 157-163.
(26) Lv, H.; Cai, Y.-B.; Zhang, J.-L. Copper-Catalyzed Hydrodefluorination of Fluoroarenes by Copper Hydride Intermediates. *Angew. Chem., Int. Ed.* **2013**, *52*, 3203-3207.
(27) Zhang, Y.; Rovis, T. A Unique Catalyst Effects the Rapid Room-Temperature Cross-Coupling of Organozinc Reagents with Carboxylic Acid Fluorides, Chlorides, Anhydrides, and Thioesters. *J. Am. Chem. Soc.* **2004**, *126*, 15964-15965.
(28) Keaveney, S. T.; Schoenebeck, F. Palladium-Catalyzed Decarbonylative Trifluoromethylation of Acid Fluorides. *Angew. Chem., Int. Ed.* **2018**, *57*, 4073-4077.
(29) Kalow, J. A.; Doyle, A. G. Enantioselective Ring Opening of Epoxides by Fluoride Anion Promoted by a Cooperative Dual-Catalyst System. *J. Am. Chem. Soc.* **2010**, *132*, 3268-3269.
(30) Wyss, C. M.; Tate, B. K.; Bacsa, J.; Wieliczko, M.; Sadighi, J. P. Dinuclear μ-fluoro cations of copper, silver and gold. *Polyhedron* **2014**, *84*, 87-95.
(31) Xu, S.; Held, I.; Kempf, B.; Mayr, H.; Steglich, W.; Zipse, H. The DMAP-Catalyzed Acetylation of Alcohols—A Mechanistic Study (DMAP=4-(Dimethylamino)pyridine). *Chem. Eur. J.* **2005**, *11*, 4751-4757.
(32) Larionov, E.; Mahesh, M.; Spivey, A. C.; Wei, Y.; Zipse, H. Theoretical Prediction of Selectivity in Kinetic Resolution of Secondary Alcohols Catalyzed by Chiral DMAP Derivatives. *J. Am. Chem. Soc.* **2012**, *134*, 9390-9399.

Insert Table of Contents artwork here

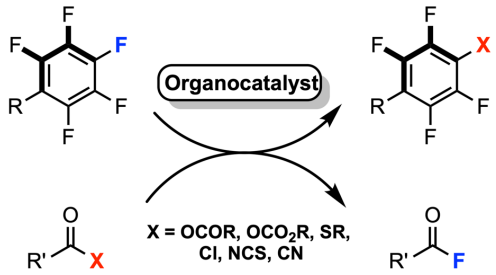

Organocatalyzed Fluoride Metathesis

Daniel Mulryan, Andrew J. P. White and Mark R. Crimmin*

Department of Chemistry, Molecular Sciences Research Hub, Imperial College London, White City, Shepherds Bush, W12 0BZ, UK

Contents:

1. Experimental Methods.

Reactions were carried out using standard Schlenk-line and glovebox techniques. All reagents were manipulated in a glovebox, with the exception of acetonitrile, which was added to reaction mixtures in a fumehood. Reactions were carried out in J. Young's tap NMR tubes. Glassware was dried for 12 hours at 120 °C prior to use. All solvents were dried over activated alumina from an SPS (solvent purification system) and subsequently degassed, prior to use. Benzene-d_6 was stored over 3 Å molecular sieves. Reactions were heated using silicone oil baths. ^{1}H, ^{13}C and ^{19}F NMR spectra were obtained on BRUKER 400 MHz or 500 MHz machines and referenced against $SiMe_4$ (^{1}H, ^{13}C) or $CFCl_3$ (^{19}F). All peak intensities are derived against an internal standard peak of 1,4-difluorobenzene (δ_F = -121.1 ppm). A 55s delay was used for quantitative ^{19}F NMR integration. NMR data was processed using MestReNova software. Multiplicity assignments in NMR spectra are labelled as follows: "s" = singlet, "d"= doublet, "t"= triplet, "m" = multiplet.

Reagents were purchased from Sigma Aldrich. All reagents were stored under an inert atmosphere, with liquid reagents being dried over activated 3 Å molecular sieves and freeze-pump-thaw degassed before use. Purifications were carried out by column chromatography on silica gel (tech grades, 60 Å, 230-400 mesh, 40-63 μm particle size) using a ratio of 9:1 parts n-pentane : DCM, or a ratio of 19:1 parts n-hexane: ethyl acetate.

2.1. Solvent Screening:

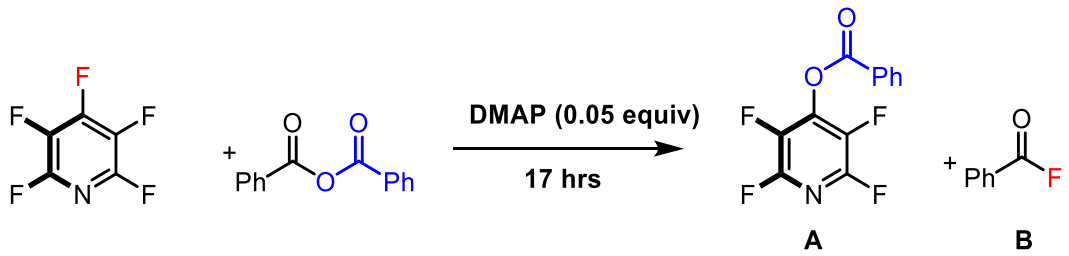

[0.14 mmol] [0.14 mmol]

Entry	Solvent	Temperature	Product A Yield (%)	Product B Yield (%)
1	$CHCl_3$	RT	32.6	0
2	THF	60	25.8	0
3	Toluene	100	31.4	18.9
4	CH_3CN	60	26.4	29.5
5	CH_3CN	80	35.4	57.4
6	CH_3CN	100	48.3	69.7
7	C_6H_5Br	150	53.4	42.7

Table S1. Reactions performed in J-Youngs NMR tubes with 1:1:0.05 equivalents of pentafluoropyridine (15.4 µl, 0.14 mmol): benzoic anhydride : DMAP in 0.4 ml of solvent, with a C_6D_6 capillary insert. 10 µl of 1,4-difluorobenzene was added as an internal standard. Yields were calculated using ^{19}F NMR.

2.2. Anhydride Equivalents Optimisation

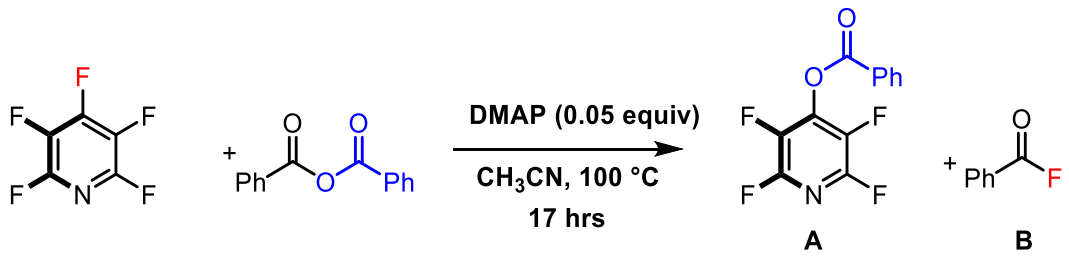

Entry	Benzoic anhydride equivalents	Product A Yield (%)	Product B Yield (%)
8	1.0	32.6	69.7
9	1.2	38.7	68.2
10	1.5	61.3	78.6
11	2.0	85.9	92.4
12	5.0	88.3	97.6
13	10.0	95.0	95.7

Table S2. Reactions performed in J-Youngs NMR tubes with 1:0.05 equivalents of pentafluoropyridine (15.4 µl, 0.14 mmol) : DMAP in 0.4 ml of acetonitrile, with a C_6D_6 capillary insert. 10 µl of 1,4-difluorobenzene was added as an internal standard. Yields were calculated using ^{19}F NMR.

2.3. Organocatalyst Screening

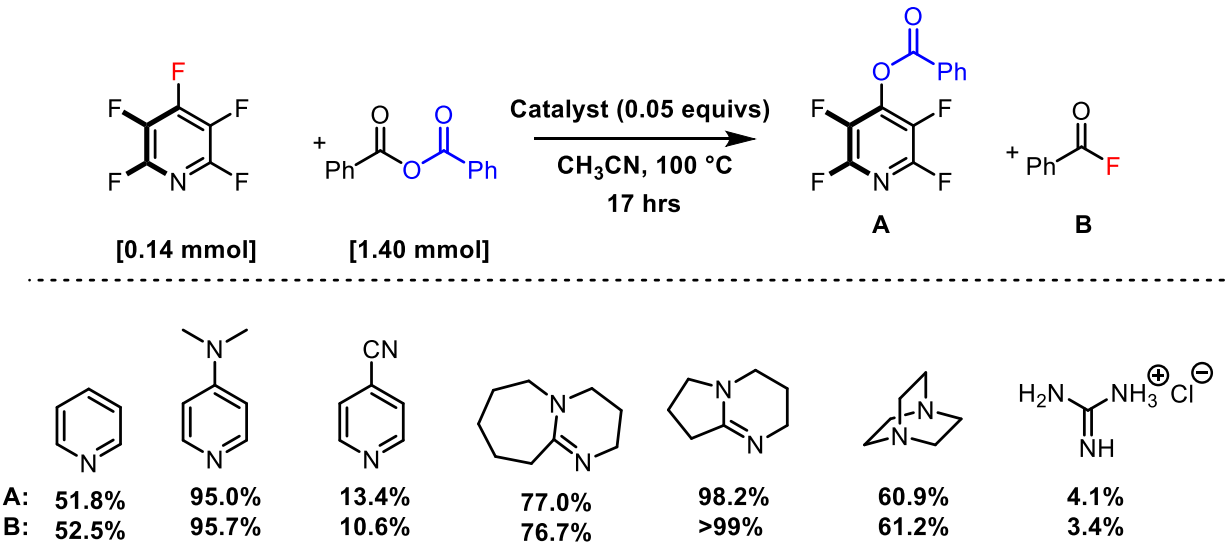

Scheme S1. Reactions performed in J-Youngs NMR tubes with 1:10:0.05 equivalents of pentafluoropyridine (15.4 µl, 0.14 mmol) : benzoic anhydride : DMAP in 0.4 ml of acetonitrile, with a C_6D_6 capillary insert. 10 µl of 1,4-difluorobenzene was added as an internal standard. Yields were calculated using ^{19}F NMR spectroscopy.

2.4. Precatalyst reactions

Catalytic amounts (5 mol%) of pyridinium salt A and B were formed, before pentafluoropyridine (0.14 mmol) and benzoic anhydride (1.40 mmol) were added. After 17 hours at 100 °C, stoichiometric conversion to products was observed in both cases.

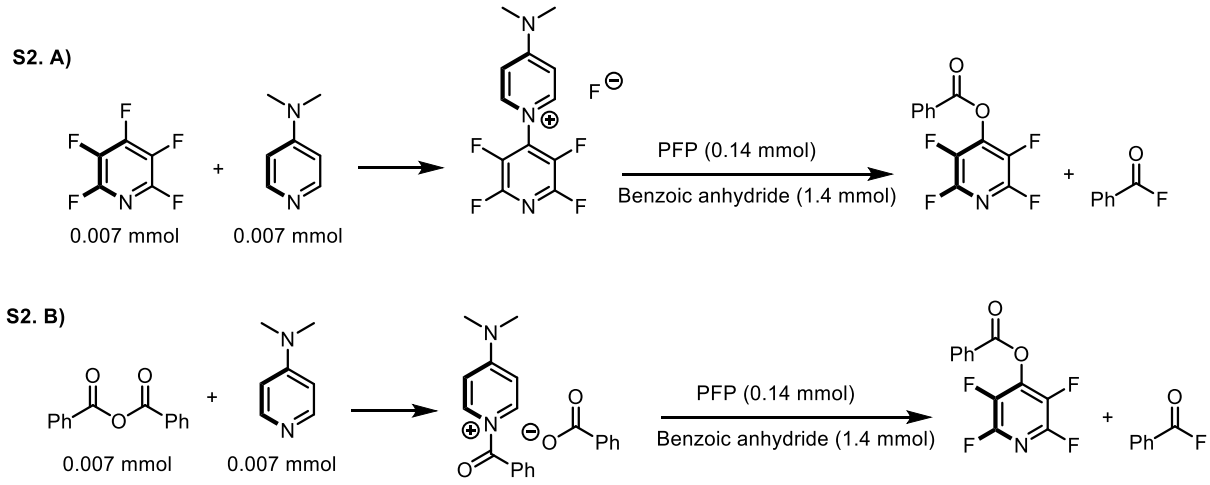

Scheme S2. Reactions performed in J-Youngs NMR tubes, in 0.4 ml of acetonitrile, with a C_6D_6 capillary insert. 10 µl of 1,4-difluorobenzene was added as an internal standard. Yields were calculated using ^{19}F NMR.

3.1. General procedure for fluorine – carbonyl shuttling reactions (1a-i).

In a glovebox, a fluoroarene (1 equivs, 0.14 mmol), the carbonyl derivative (10 equiv., 1.40 mmol) and 1,4-difluorobenzene (10 µl, 0.097mmol) were added to an empty J. Young's NMR tube. The reaction mixture was removed from the glovebox before 0.4 ml of dry acetonitrile was added. A stock solution of 4-N,N-dimethylaminopyridine (DMAP) was made by dissolving 30 mg of DMAP in 4 ml of dry C_6D_6. Once a 0 hrs time-point has been taken by ^{19}F NMR, 50 µl of this stock solution (0.05 equiv., 0.007 mmol) was added to the reaction mixture. The NMR tube was sealed and heated at 100 °C for 17 hours in a silicone oil bath. Quantitative ^{19}F integration was performed using the 1,4-difluorobenzene singlet resonance at δ_F -121.1 ppm.

Scaled up versions of each reaction were also conducted. In a glovebox pentafluoropyridine (154 µl, 1 equiv., 1.4 mmol), the carbonyl derivative (10 equiv., 14.0 mmol), DMAP (0.05 equiv. 0.07 mmol) and a stirrer bar were added to an empty 25 ml ampoule. The ampoule was removed from the glovebox and 5 ml of dry acetonitrile was added. The reaction mixture was stirred and heated to 100 °C for 17 hours in a silicone oil bath. Isolated yields were achieved by scaling up reactions and isolating products via column chromatography. The synthesis of **1g** was conducted in bromobenzene solvent at 150 °C for 17 hours rather than acetonitrile at 100 °C for both NMR tube and scaled up reactions. The synthesis of **1m** and **1n** were conducted with 0.05 equivalents of 1,8-Diazabicyclo[5.4.0]undec-7-ene (DBU) catalyst, instead of DMAP.

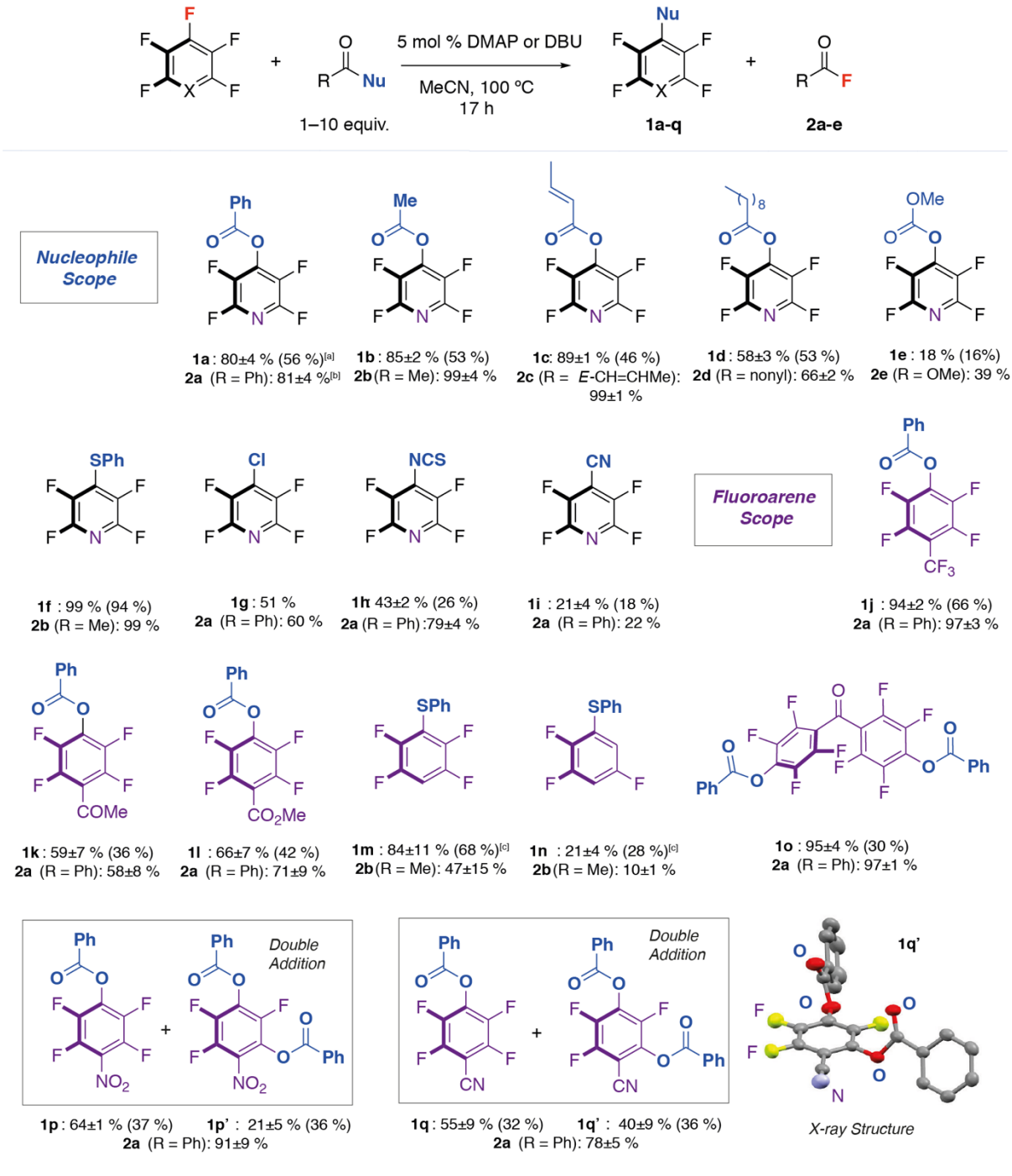

Table S1 Fluoride metathesis reaction of pentafluoropyridine with a range of different carbonyl derived functional groups

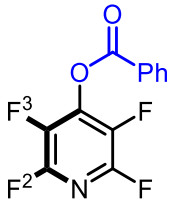

1a. 4-benzoic-2,3,5,6-tetrafluoropyridine: Isolation achieved by column chromatography in 7:3 n-hexane: dichloromethane, R_F = 0.45. (213 mg, 56.1 %, 0.79 mmol).

δ_H (400 MHz, C_6D_6, 298K): 7.932 (d, 2H, $^3J_{HH}$=7.2, o-CH), 7.08 (t, 1H, $^3J_{HH}$=7.8, p-CH), 6.94 (t, 2H, $^3J_{HH}$=8.0, m-CH).

δ_C (100 MHz, C_6D_6, 298K): 160.9 (s, 1C, OCOPh), 144.6 (dm, 2C, $^1J_{CF}$ = 243 Hz, CF^2), 139.3 (m, 1C, CO), 137.6 (dm, 2C, $^1J_{CF}$ = 262 Hz, CF^3), 134.5 (s, 2C,o-CH), 130.6 (s, 1C, p-CH), 128.7 (s, 2C, m-CH) 126.2 (s, 1C, i-C)

δ_F (100 MHz, C_6D_6, 298K): -88.9 (m, 2F, CF^2), -152.5 (m, 2F, CF^3).

IR (cm^{-1}): 1770.5 (C=O str), 1282.2 (C-O str), 1233.7 (C-O str).

MS (APCL): Molecular ion not observed. $C_7H_5O^+$; $[M]^+$-C_5NOF_4 (100%) 105.0 (meas).

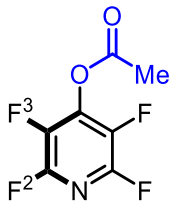

1b. 4-acetyl-2,3,5,6-tetrafluoropyridine: Isolation achieved by column chromatography in 4: 1 pentane: dichloromethane to yield product as a colourless oil. R_F = 0.65. (155 mg, 52.5. %, 0.74 mmol).

δ_H (400 MHz, C_6D_6, 298K): 4.34 (s, 3H, CH_3).

δ_C (100 MHz, C_6D_6, 298K): 164.3 (s, 1C, O<u>C</u>OCH_3), 144.5 (dm, 2C, $^1J_{CF}$ = 244 Hz, CF(2)), 137.3 (dm, 2C, $^1J_{CF}$ = 262 Hz, CF(3)), 18.3 (s, 1C, CH_3). Ipso-carbon resonance not observed

δ_F (100 MHz, C_6D_6, 298K): -89.1 (m, 2F, CF(2)), -153.3 (m, 2F, CF(3)).

MS (APCL):$C_7H_3F_4NO_2$; $[M\text{-}H]^+$ (21 %) 210.0517 (meas), 210.0103 (calc).

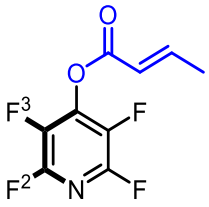

1c. 4-Crotoic-2,3,5,6-tetrafluoropyridine: Isolation achieved by column chromatography in 9: 1 n-hexane: dichloromethane to yield product as a yellow oil. R_F = 0.35. (153 mg, 46.2 %, 0.65 mmol).

δ_H (400 MHz, C_6D_6, 298K): 6.87-6.78 (dq, 1H, $^3J_{HH\text{-trans}}$ = 16.2 Hz, $^3J_{HH}$ = 7.1 Hz, CHC<u>H</u>CH_3), 5.55 (d, 1H, $^3J_{HH\text{-trans}}$ = 16.2 Hz, C<u>H</u>$CHCH_3$) 1.25 (d, 3H, $^3J_{HH}$ = 7.1 Hz, $CHCHC\underline{H}_3$).

δ_C (100 MHz, C_6D_6, 298K): 160.0 (s, 1C, O<u>C</u>$OCHCHCH_3$), 151.5 (s, 1C, $OCOCH\underline{C}HCH_3$), 144.52 (dm, 2C, $^1J_{CF}$ = 243 Hz, CF^2), 139.4 (m, 1C, C(4)), 137.7 (dm, 2C, $^1J_{CF}$ = 268 Hz, CF^3), 118.4 (s, 1C, $OCO\underline{C}HCHCH_3$), 17.6 (s, 1C, CH_3). Ipso carbon not observed.

δ_F (100 MHz, C_6D_6, 298K): -89.3 (m, 2F, CF^2), -153.0 (m, 2F, CF^3).

IR (cm^{-1}): 1763.0 (C=O str), 1297.1 (C-O str), 1200.2 (C-O str).

MS (APCL): $C_9H_6F_4NO_2$; $[M\text{-}H]^+$ (09 %) 236.0332 (meas), 236.0329 (calc).

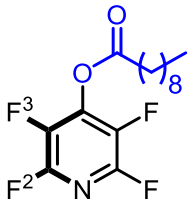

1d. 4-decanoic-2,3,5,6-tetrafluoropyridine: (98 mg, 22.6 %, 0.32 mmol). Isolation achieved by column chromatography in 9: 1 n-hexane: dichloromethane. R_F = 0.27

δ_H (400 MHz, C_6D_6, 298K): 2.06 (t, 2H, $^3J_{HH}$ = 7.55 Hz, COC$\underline{H}_2$R), 1.35-1.15 (series of m, 14H, 0.92 (t, 3H, $^3J_{HH}$ = 7.05 Hz, CH_3).

δ_C (100 MHz, C_6D_6, 298K): 167.6 (s, 1C, O$\underline{C}$OR), 144.5 (dm, 2C, $^1J_{CF}$ = 224 Hz, CF^2), 137.2 (dm, 2C, $^1J_{CF}$ = 247 Hz, CF^3), 32.7 (s, 1C, CH_2), 32.0 (s, 1C, CH_2), 29.7 (d, 1C, $^2J_{CH}$ = 5.75 Hz, CH_2), 29.4 (d, 1C, $^3J_{CH}$ = 3.55 Hz, CH_2), 29.1 (s, 1C, CH_2), 28.6 (s, 1C, CH_2), 24.4 (s, 1C, CH_2), 22.8 (s, 1C, CH_2), 14.0 (s, 1C, CH_3). Ipso carbon not observed.

δ_F (100 MHz, C_6D_6, 298K): -88.9 (m, 2F, CF^2), -153.0 (m, 2F, CF^3).

IR (cm^{-1}): 1796.6 (C=O str), 1274.7 (C-O str).

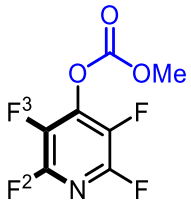

1e. methyl-2,3,4,5-tetrafluoropyridin-4-ylcarbonate: Isolation achieved by column chromatography in 9:1 n-hexane : ethyl acetate, R_F = 0.56. (61.8 mg, 19.6 %, 0.27 mmol).

δ_H (400 MHz, C_6D_6, 298K): 3.04 (s, 1H, CH_3).

δ_C (100 MHz, C_6D_6, 298K): 150.2 (s, 1C, OCOMe), 144.4 (dm, 2C, $^1J_{HF}$ = 246.7 Hz, CF^2), 138.2 (dm, 2C, $^1J_{HF}$ = 241.8 Hz, CF^3), 56.1 (s, 1C, CH_3). Ipso carbon not observed.

δ_F (100 MHz, C_6D_6, 298K): -90.85 (m, 2F, CF^2), -154.65 (m, 2F, CF^3).

MS (APCL): $C_7H_3F_4NO_3$; $[M-H]^+$ (36 %) 226.1318 (meas) 226.0204 (calc).

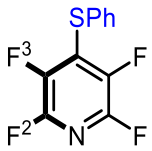

1f. 4-phenylthio-2,3,5,6-tetrafluoropyridine: Isolation achieved by column chromatography in 9:1 pentane : dichloromethane to yield a colourless oil, R_F = 0.40. (341 mg, 94.1 %,1.32 mmol).

δ_H (400 MHz, C_6D_6, 298K): 7.10 (d, 2H, $^3J_{HH}$=6.7, o-CH), 6.90 (s, 1H, p-CH), 6.88-6.83 (m, 2H, m-CH).

δ_C (100 MHz, C_6D_6, 298K): 143.3 (dm, 2C, $^1J_{CF}$ = 228 Hz, CF^2), 140.8 (dm, 2C, $^1J_{CF}$ = 232 Hz, CF^3), 132.5 (s, 2C, o-CH), 129.3 (s, 1C, p-CH), 128.9 (s, 2C, m-CH). Ipso-carbon resonances not observed.

δ_F (100 MHz, C_6D_6, 298K): -90.9 (m, 2F, CF^2), -136.6 (m, 2F, CF^3).

MS (APCL): $C_{12}H_3F_4NO_2$; $[M-H]^+$(24 %) 242.0620 (meas) 242.0518 (calc).

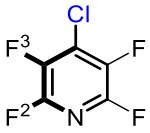

1g. 4-chloro-2,3,5,6-tetrafluoropyridine:

δ_F (100 MHz, C_6D_6, 298K): -90.63 (m, 2F, CF^2), -142.60 (m, 2F, CF^3) in close agreement with the current literature.[S1]

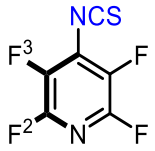

1h. 4-isothiocyanato-2,3,5,6-tetrafluoropyridine: Isolation achieved by column chromatography in 9:1 n-hexane : ethyl-acetate, R_F = 0.44. (75.4 mg, 25.9%, 0.36 mmol).*

δ_C (100 MHz, C_6D_6, 298K): 148.1 (s, 1C, NCS), 143.1 (dm, 2C, $^1J_{CF}$ = 237 Hz, CF^3), 140.1 (dm, 2C, $^1J_{CF}$ = 240 Hz, CF^2), 128.5 (s, 1C, CNCS).

δ_F (100 MHz, C_6D_6, 298K): -91.4 (m, 2F, CF^2), -133.9 (m, 2F, CF^3).

IR (cm^{-1}): 1916 (NCS str).

MS (APCL): Molecular ion not observed. $C_5F_4NS^{+\cdot}$; $[M]^+$-CN (100%) 181.9687 (meas). 181.9850 (calc).

*The SCN^- anion is ambiphilic and can potentially perform S_NAr from either the S^- or N^- positions. 4-thiocyanato-2,3,5,6-tetrafluoropyridine is characterised by a nitrile carbon environment at approximately 110 ppm, and a CN stretch at approximately 3150 cm^{-1}.[S2] 4-isothiocyanato-2,3,5,6-tetrafluopyridine is characterised by a NCS carbon environment at 148.1 ppm and a NCS stretch at 1916 cm^{-1}.[S3]

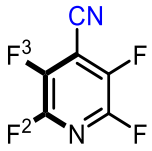

1i. 4-cyano-2,3,5,6-tetrafluoropyridine: Isolation achieved by column chromatography in 9:1 n-pentane: dichloromethane, R_F = 0.57. (45 mg, 18.2%, 0.26 mmol).

δ_C (100 MHz, C_6D_6, 298K): 143.6 (s, 2C, CF^2), 136.4 (s, 2C, CF^3), 112.9 (s, 1C, CN), 110.0 (s, 1C, i-C).

δ_F (100 MHz, C_6D_6, 298K): -88.6 (m, 2F, CF^2), -153.2 (m, 2F, CF^3).

IR (cm^{-1}): 3092.4 (N-H amide str), 1684.8 (C=O amide str) – suggests nitrile hydrolysis to amide.*

MS (APCL): Molecular ion not observed. $C_6NFO_4^+$ $[M]^+ + H_2O - NH_2$ (15%) 178.0232 (meas).

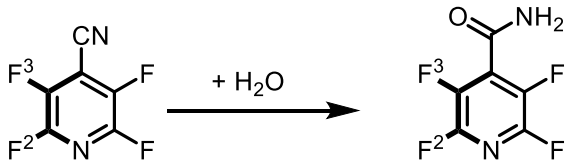

*It is proposed that hydrolysis of species 1i occurred before IR and mass spectroscopy were taken, consistent with the observation of amide N–H and C=O stretches in the IR spectrum, and the detection of a $C_6NFO_4^+$ ion in mass spectroscopy.

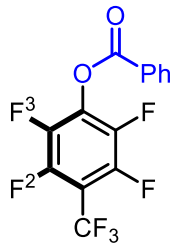

1j 4-benzoic-2,3,5,6-tetrafluorooctofluorotoluene: Isolation achieved by column chromatography in 2:1 hexane: dichloromethane, R_F = 0.40 (309 mg, 65.8 %, 0.92 mmol).

δ_H (400 MHz, C_6D_6, 298K): 7.99 (d, 2H, $^3J_{HH}$ = 7.94 Hz, o-CH), 7.08 (t, 1H, $^3J_{HH}$ = 7.45 p-CH), 6.95 (t, 2H, $^3J_{HH}$ = 7.62 m-CH).

δ_C (100 MHz, C_6D_6, 298K): 161.6 (s, 1C, OCOPh), 145.6 (dm, 2C, $^1J_{CF}$ = 264 Hz, CF^2), 142.4 (dm, 2C, $^1J_{CF}$ = 244 Hz, CF^3), 134.4 (s, 2C, o-CH), 132.6 (m, 1C, C^4), 130.5 (s, 1C, p-CH), 128.6 (s, 2C m-CH), -126.5 (s, 1C, i-C), -120.9 (s, 1C, CF_3). Ipso carbon C^1 not observed.

δ_F (100 MHz, C_6D_6, 298K): -55.8 (t, 3F, $^2J_{FF}$ = 21.9 Hz, CF_3), -141.0 (m, 2F, CF^2), -150.9 (m, 2F, CF^3).

IR (cm^{-1}): 1766.8 (C=O str), 1271.0 (C-O str), 1207.7 (C-O str).

MS (APCL): $C_{14}H_5F_7O_2$; $[M-H]^+$ (99 %) 339.0249 (meas), 339.0251 (calc).

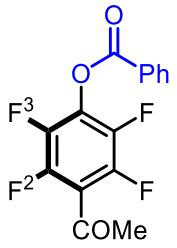

1k, 4-benzoic-2,3,5,6-tetrafluoroacetophenone Isolation achieved by column chromatography in 9: 1 hexane: dichloromethane to yield product as a white solid. R_F = 0.50. (159 mg, 36.1 %, 0.51 mmol).

δ_H (400 MHz, C_6D_6, 298K): 8.02 (d, 2H, $^3J_{HH}$ = 8.1, o-CH), 7.08 (t, 1H, $^3J_{HH}$ = 7.6, p-CH), 6.95 (t, 2H, $^3J_{HH}$ = 8.2 m-CH), 1.94 (m, 3H, $COCH_3$).

δ_C (100 MHz, C_6D_6, 298K): 189.7 (s, 1C, COCH3), 162.1s, 1C, OCOPh),150.4 (dm, 2C, $^1J_{CF}$ = 260 Hz), 145.6 (dm, 2C, $^1J_{CF}$ = 256 Hz), 134.2 (s, 2C, o-CH), 130.5 (s, 2C, p-CH), 128.6 (s, 2C m-CH), 126.8 (s, 1C, i-CH), 31.4 (s, 1C, CH_3).

δ_F (100 MHz, C_6D_6, 298K): -142.3 (m, 2F, CF^2), -152.3 (m, 2F, CF^3).

IR (cm^{-1}): 1759.3 (C=O ester str), 1699.7 (C=O ketone str), 1312.0 (C-O str), 1241.2 (C-O str).

MS (APCL): $C_{15}H_9F_4O_3$; $[M-H]^+$ (99 %) 313.0479 (meas), 313.0482 (calc).

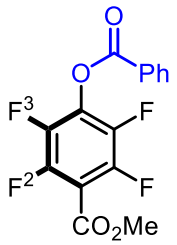

1l, 4-benzoic-2,3,5,6-tetrafluoromethylbenzoate Isolation achieved by column chromatography in 95:5 pentane: ethyl acetate, to yield product as a white solid. R_F = 0.46 (197 mg, 42.4 %, 0.60 mmol).

δ_H (400 MHz, C_6D_6, 298K): 8.00 (d, 2H, $^3J_{HH}$ = 7.1, o-CH), 7.04 (t, 1H, $^3J_{HH}$ =7.3, p-CH), 6.93 (t, 2H, $^3J_{HH}$ = 7.6, m-CH), 3.33 (s 3H CO_2CH_3).

δ_C (100 MHz, C_6D_6, 298K): 161.9 (s, 1C, O<u>C</u>OPh), 145.5 (m, 2C, CF^2 via HSQC), 141.7 (m, 2C, CF^3 via HSQC), 134.2 (s, 2C, o-CH), 130.5 (m, 1C, p-<u>C</u>OCOPh), 128.6 (s, 1C, p-CH), 128.6 (s, 2C m-CH), 126.8 (s, 1C, <u>C</u>CO_2CH_3), 52.2 (s, 1C , CO_2<u>C</u>H_3). Ipso carbon not observed.

δ_F (100 MHz, C_6D_6, 298K): -146.9 (m, 2F, CF^2), -149.9 (m, 2F, CF^3)

IR (cm^{-1}): 1766.8 (C=O ester str), 1729.5 (C=O acid str), 1323.2 (C-O acid str), 1218.8 (C-O ester str), 1103.3 (C-O ester str)

MS (APCL): $C_{15}H_9F_4O_4$; $[M-H]^+$ (27 %) 329.0432 (meas), 329.0431 (calc).

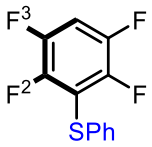

1m, phenyl-2,3,5,6-tetrafluorophenylsulfane: Isolation achieved by column chromatography in 19:1 n-hexane : dichloromethane to yield product as a colourless oil. R_F = 0.69 (244.2 mg, 67.6 %, 0.95 mmol).

δ_H (400 MHz, C_6D_6, 298K):7.20-7.17 (m, 2H, m-CH), 6.85 (d, 1H, $^3J_{HH}$=1.82 Hz, p-CH), 6.83 (d, 1H, $^3J_{HH}$=1.82 Hz), 6.11-6.03 (m, 1H, CH^1).

δ_C (100 MHz, C_6D_6, 298K): 147.54 (dm, 2C, $^1J_{CF}$=102.24 Hz, CF^2), 145.07, (dm, 2C, $^1J_{CF}$=107.79 Hz, CF^3), 134.38 (s, 1C, i-C), 130.47 (s, 2C, o-CH), 129.2 (s, 2C, m-CH), 128.95 (s, 1C, p-CH), 106.58 (t, 1C, $^2J_{CF}$=27.54 Hz, CH^4). Ipso carbon (CS^1) not observed.

δ_F (100 MHz, C_6D_6, 298K):-134.4 (m, 2F, CF^2), -138.9 (m, 2F, CF^3)

MS (APCL): $C_{12}H_6F_4S$; $[M-H]^+$ (95 %) 259.0197 (meas), 259.0191 (calc).

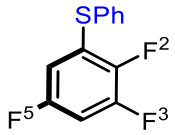

1n, phenyl-2,3,5-trifluorophenylsulfane: Isolation achieved by column chromatography in 19:1 n-hexane : dichloromethane to yield product as a colourless oil. R_F = 0.69 (96.8 mg, 28.7 %, 0.40 mmol).

δ_H (400 MHz, C_6D_6, 298K):7.17 (d, 1H, $^3J_{HH}$=1.99 Hz, p-CH), 6.88 (d, 2H, $^3J_{HH}$=1.82 Hz, m-CH), 6.87 (d, 2H, $^3J_{HH}$=2.12 Hz, o-CH), 6.33-6.28 (m, 1H, CH^6), 6.14-6.07 (m, 1H, CH^4).

δ_C (100 MHz, C_6D_6, 298K): 157.63 (d, 1C, $^1J_{CF}$ = 247.8 Hz, CF^2), 201.91 (d, 1C, $^1J_{CF}$ = 247.5 Hz, CF^3), 182.15 (d, 1C, $^1J_{CF}$ = 226.8 Hz, CF^5), 133.26 (s, 2C, o-CH), 129.53 (s, 2C, m-CH), 128.95 (s, 1C, C^1), 128.61 (s, 1C, p-CH), 126.87 (s, 1C, i-C), 111.74-111.47 (m, 1C, CH^6), 103.51-103.02 (m, 1C, CH^4).

δ_F (100 MHz, C_6D_6, 298K): -115.2 (m, 1F, CF^5), -134.2 (m, 1F, CF^3), -141.6 (m, 1F, CF^2).

MS (APCL): $C_{12}H_7F_3S^+$; $[M-H]^+$ (99 %) 241.0289 (meas), 241.0293 (calc).

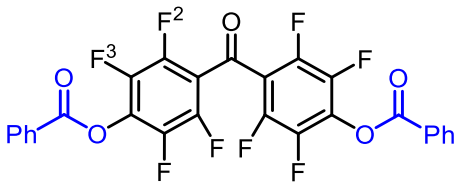

1o, 4,4-dibenzoic octofluorobenzophenone: Isolation achieved by column chromatography in 9:1 hexane:dichloromethane to yield product as a white solid. R_F = 0.29 (236 mg, 29.8 %, 0.42 mmol).

δ_H (400 MHz, C_6D_6, 298K): 8.00 (d, 4H, $^3J_{HH}$ = 8.1 Hz, o-CH), 7.07 (t, 2H, $^3J_{HH}$ = 7.8 Hz p-CH), 6.94 (t, 4H, $^3J_{HH}$ = 7.5 Hz, m-CH).

δ_C (100 MHz, C_6D_6, 298K): 144.8 (m, 4C, CF^2 via HSQC), 141.2 (m, 4C, CF^3 via HSQC), 134.2 (s, 4C, o-CH), 130.6 (s, 2C, p-CH), 128.6 (s, 4C m-CH).

δ_F (100 MHz, C_6D_6, 298K): -142.4(m, 4F, CF^2), -150.9 (m, 4F, CF^3)

MS (APCL): $C_{27}H_{10}F_8O_5$; $[M-H]^+$ (6 %) 567.0471 (meas), 567.0473 (calc).

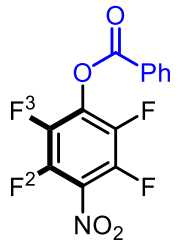

1p 4-benzoic-2,3,5,6-tetrafluoronitrobenzene: Isolation achieved by column chromatography in 95:5 n-hexane: ethyl acetate, R_F = 0.43 (164 mg, 37.3 %, 0.52 mmol).

δ_H (400 MHz, C_6D_6, 298K): 7.96 (d, 2H, $^3J_{HH}$=8.47 Hz, o-CH), 7.07 (t, 1H, $^3J_{HH}$=8.02 Hz, p-CH), 6.94 (t, 2H, $^3J_{HH}$=8.11, m-CH).

δ_C (100 MHz, C_6D_6, 298K): 161.4 (s, 1C, O<u>C</u>OPh), 142.1 (m, 2C, CF(2)), 139.5 (m, 2C, CF(3)), 134.6 (s, 2C, o-CH), 130.5 (m, 1C, C^4O), 128.7 (s, 1C, p-CH), 128.6 (s, 2C m-CH), 126.3 (s, 1C, i-C). Ipso carbon C^1 not observed.

δ_F (100 MHz, C_6D_6, 298K): -146.9 (m, 2F, CF^2), -149.9 (m, 2F, CF^3)

IR (cm^{-1}): 1766.8 (C=O str), 1550.6 (N=O assym.str), 1356.8 (N=O sym.str), 1233.7 (C-O str), 1107.0 (C-O str).

MS (APCL): $C_{13}H_6F_4NO_4$; $[M-H]^+$ (14 %) 316.0228 (meas), 316.0227 (calc).

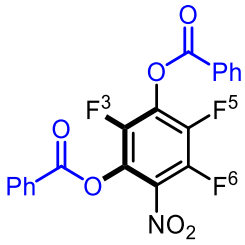

1p' 2,4-dibenzoic-3,5,6-trifluorobenzonitrile: Isolation achieved by column chromatography in 95:5 hexane: ethyl acetate, R_F = 0.26. (87.8 mg, 36.2%, 0.21 mmol).

δ_H (400 MHz, C_6D_6, 298K): 7.95 (d, 4H, $^3J_{HH}$ = 7.8 Hz, o-CH) , 7.08 (t, 2H, $^3J_{HH}$ = 7.4 Hz p-CH), 6.95 (t, 4H, $^3J_{HH}$ = 7.7 Hz m-CH).

δ_C (100 MHz, C_6D_6, 298K): 162.3 (s, 1C, 4-O<u>C</u>OPh), 161.7 (s, 1C, 2-O<u>C</u>OPh), 145.5 (1C, m, CF^6 via HSQC), 142.9 (1C, m, CF^5 via HSQC), 141.7 (1C, m, CF^3 via HSQC), 134.4 (d, 1C, $^3J_{CH}$=11 Hz, o-CH), 133.8 (s, 1C, o-CH), 130.6 (s, 1C, p-CH), 130.3 (s, 1C, p-CH), 128.6 (s, 1C, m-CH), 128.5, (s,1C, m-CH), 126.6 (s, 1C, i-CH), 126.5 (s,1C, i-CH). Ipso carbons not observed.

δ_F (100 MHz, C_6D_6, 298K): -139.7 (d, 1F, $^3J_{FF}$ = 8.3 Hz, CF^6), -146.1 (d, 1F, $^3J_{FF}$ = 23.7 Hz CF^5), -146.5 (dd, 1F, CF^3).

IR (cm^{-1}): 1759.3 (C=O str), 1714.6 (C=O str), 1550.6 (N=O assym.str), 1356.8 (N=O sym.str), 1207.7 (C-O str), 1170.4 (C-O str), 1103.3 (C-O str).

MS (APCL): $C_{20}H_{10}F_3NO_6Na$; $[M + Na]^+$ (65 %) 440.0357 (meas), 440.0352 (calc).

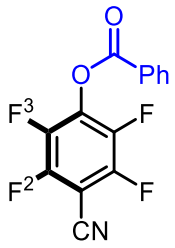

1q, 4-benzoic-2,3,5,6-tetrafluorobenzonitrile: Isolation achieved by column chromatography in 9: 1 n-pentane: ethyl acetate, R_F = 0.55. (131 mg, 31.5 %, 0.44 mmol).

δ_H (400 MHz, C_6D_6, 298K): 7.97 (d, 2H, $^3J_{HH}$ = 7.6 Hz, o-CH) , 7.13 (t, 1H, $^3J_{HH}$ = 7.6 Hz, p-CH), 7.01 (t, 2H, $^3J_{HH}$ = 8.5 Hz, m-CH).

δ_C (100 MHz, C_6D_6, 298K): 161.5(s, 1C, O<u>C</u>OPh), 147.5 (m, 2C, CF^2 via HSQC), 141.0 (m, 2C, CF^3 via HSQC), 134.5 (s, 2C, o-CH), 130.5 (s, 1C, p-CH), 128.7 (s, 2C m-CH) 126.3 (s, 1C, benzoyl i-C). Ipso carbons not observed, nitrile carbon not observed.

δ_F (100 MHz, C_6D_6, 298K): -133.5 (m, 2F, CF^2), -150.3 (m, 2F, CF^3).

IR (cm^{-1}): 2231.5 (CN str), 1766.8 (C=O str), (1233.7 C-O str), (1118.2 CO str).

MS (APCL): $C_{14}H_5F_4NO_2$; $[M-H]^+$ (63 %) 296.0332 (meas), 296.0329 (calc).

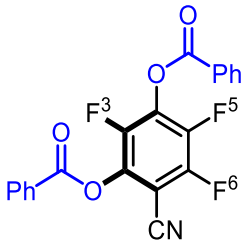

1q', 2,4-dibenzoic-3,5,6-trifluorobenzonitrile: Isolation achieved by column chromatography in 9:1 n-pentane: ethyl acetate, R_F = 0.30 (199 mg, 35.9 %, 0.50 mmol).

δ_H (400 MHz, C_6D_6, 298K): 7.95 (d, 4H, $^3J_{HH}$ = 7.9 Hz, o-CH) , 7.08 (t, 2H, $^3J_{HH}$ = 7.2 Hz, p-CH), 6.95 (t, 4H, $^3J_{HH}$ = 7.7 Hz, m-CH).

δ_C (100 MHz, C_6D_6, 298K): 162.1 (s, 1C, 4-O<u>C</u>OPh), 161.7 (s, 1C, 2-O<u>C</u>OPh), 153.3 (dm, 1F, $^1J_{CF}$ = 261 Hz, CF^6), 148.6 (dm, 1F, $^1J_{CF}$ = 260 Hz, CF^5), 145.8 (dm, 1F, $^1J_{CF}$ = 263 Hz, CF^3), 134.3 (s, 2C, o-CH), 133.8 (s, 2C, o-CH), 130.6, (s, 1C, p-CH), 130.4 (s, 1C, p-CH), 128.7 (s, 2C, m-CH), 128.5 (s, 2C, m-CH), 126.7 (s, 1C, i-C), 126.5 (s, 1C, i-C) 108.1 (s, 1C, CN).

δ_F (100 MHz, C_6D_6, 298K): -132.5 (m, 1F, CF^3), -139.4 (d, 1F, $^3J_{FF}$=10.96 Hz, CF^5), -147.0 (d, 1F, $^3J_{FF}$=21.14, CF^6).

IR (cm^{-1}): 2170.4 (CN str), 1774.2 (C=O str), 1714.6 (C=O str), 1207. 7 (C-O str), 1170.4, (C-O str), 1036.2 (C-O str).

MS (APCL): $C_{21}H_{11}F_3NO_4$; $[M-H]^+$ (99 %) 398.0631 (meas), 398.0635 (calc).

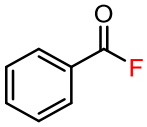

2a Benzoyl fluoride: Isolation achieved by column chromatography in 7:3 hexane: dichloromethane, R_F = 0.72. (126.1 mg, 72.6 %, 1.02 mmol).

δ_H (400 MHz, C_6D_6, 298K): 7.67 (d, 2H, $^3J_{HH}$ = 7.7 Hz, o-CH), 6.99 (t, 1H, $^3J_{HH}$ = 7.5 Hz, p-CH), 6.82 (t, 2H, $^3J_{HH}$ = 8.6 Hz, m-CH).

δ_C (100 MHz, C_6D_6, 298K): 158.7 (d, 1C, $^1J_{CF}$ = 342 Hz, COF), 134.5 (s, 2C, o-CH), 131.0 (s, 1C, p-CH), 128.5 (s, 2C, m-CH). Ipso carbon not observed.

δ_F (00 MHz, C_6D_6, 298K): 17.9 (s, 1F).

2b Acetyl fluoride:

δ_F (100 MHz, C_6D_6, 298K): 50.5 (s, 1F) in close agreement with the current literature.[4]

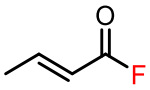

2c Crotonyl fluoride:

δ_F (100 MHz, C_6D_6, 298K): 23.0 (s, 1F)

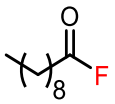

2d Decanoyl fluoride:

δ_F (100 MHz, C_6D_6, 298K): 43.4 (s, 1F) in close agreement with the current literature. [5]

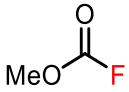

2e Methyl carbonofluoridate:

δ_F (100 MHz, C_6D_6, 298K): -20.0 (s, 1F) in close agreement with the current literature.[6]

4. X-ray Crystal Structures.

The X-ray crystal structure of 1k

Crystal data for **1k**: $C_{15}H_8F_4O_3$, M = 312.21, monoclinic, $C2/c$ (no. 15), a = 25.3257(12), b = 5.9112(3), c = 17.3301(9) Å, β = 97.384(5)°, V = 2572.9(2) Å^3, Z = 8, D_c = 1.612 g cm^{-3}, μ(Mo-Kα) = 0.150 mm^{-1}, T = 173 K, colourless tablets, Agilent Xcalibur 3 E diffractometer; 2587 independent measured reflections (R_{int} = 0.0159), F^2 refinement,[5,6] R_1(obs) = 0.0366, wR_2(all) = 0.0938, 2117 independent observed absorption-corrected reflections [$|F_o| > 4\sigma(|F_o|)$, completeness to θ_{full}(25.2°) = 98.6%], 201 parameters. CCDC 2021812.

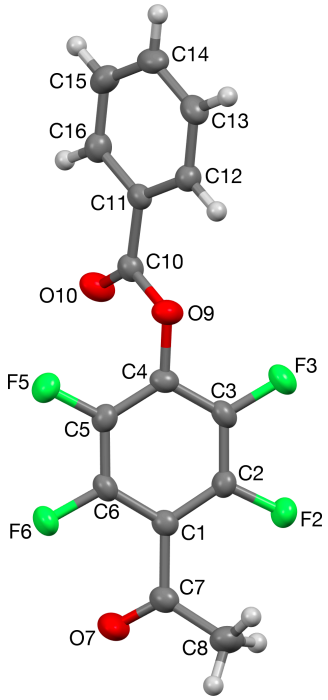

Figure S1. The crystal structure of **1k** (50% probability ellipsoids).

The X-ray crystal structure of 1q'

Crystal data for **1q'**: $C_{21}H_{10}F_3NO_4$, M = 397.30, monoclinic, $P2_1/c$ (no. 14), a = 17.0077(5), b = 7.5346(2), c = 13.5271(4) Å, β = 92.463(3)°, V = 1731.84(9) Å^3, Z = 4, D_c = 1.524 g cm^{-3}, μ(Mo-Kα) = 0.127 mm^{-1}, T = 173 K, colourless blocky needles, Agilent Xcalibur 3 E diffractometer; 3896 independent measured reflections (R_{int} = 0.0354), F^2 refinement,[S5],[S6] R_1(obs) = 0.0452, wR_2(all) = 0.1089, 2598 independent observed absorption-corrected reflections [$|F_o| > 4\sigma(|F_o|)$, completeness to θ_{full}(25.2°) = 100%], 262 parameters. CCDC 2021813.

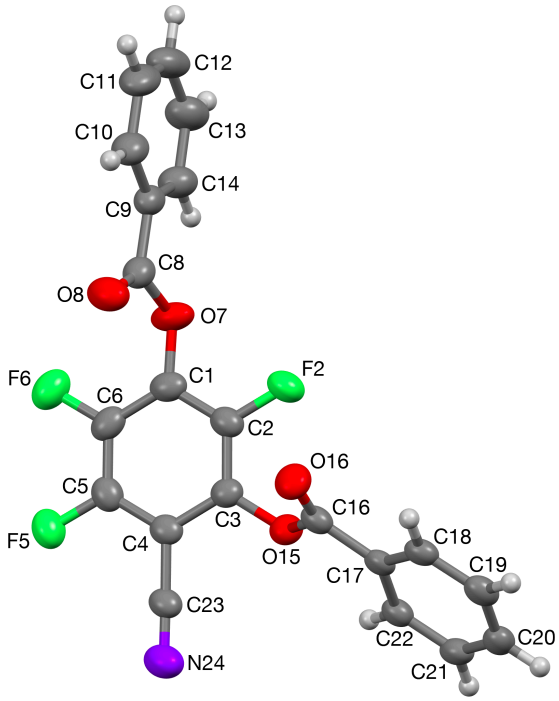

Figure S2. The crystal structure of **1q'** (50% probability ellipsoids).

5. DFT studies

5.1 Dual Catalysed Pathway

DFT calculations were run using Gaussian 09 (Revision D.01) using the B3LYP, B3PW91 and ωB97X-D density functionals. The 6-31G** basis set was used for all atoms. Geometry optimisation calculations were performed without symmetry constraints. Frequency analyses for all stationary points were performed to confirm the nature of the structures as either minima (no imaginary frequency) or transition states (only one imaginary frequency). Intrinsic reaction coordinate (IRC) calculations followed by full geometry optimisations on final points were used to connect transition states and minima located on the potential energy surface allowing a full energy profile (calculated at 298.15 K, 1 atm) of the reaction to be constructed. Free energies reported are corrected for the effects of acetonitrile (Ɛ=36.64) solvent using the polarizable continuum model (PCM). Calculations run using the B3LYP or B3PW91 functionals were corrected with GD3-BJ empirical dispersion inclusion. The graphical user interface used to visualise the various properties of the intermediates and transition states was GaussView 5.0.9.

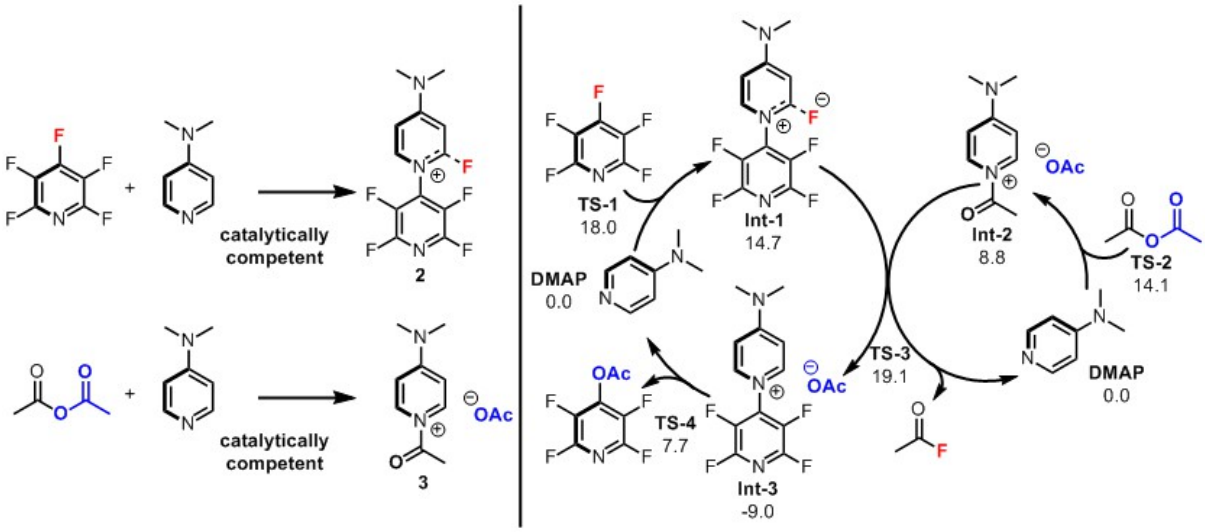

	B3LYP (Kcal mol^{-1})	B3PW91 (Kcal mol^{-1})	WB97X-D (Kcal mol^{-1})
TS-1	18.0	17.9	21.6
Int-1	14.7	14.3	15.8
TS-2	14.1	13.6	16.5
Int-2	8.8	9.7	11.6
TS-3	19.1	25.1	27.6
Int-3	-9.0	-9.2	-9.5
TS-4	7.7	8.7	9.5
Product	-5.8	-6.3	-6.0

Table S3. Functional testing for the energy profile of the dual-catalysed reaction, shown in Figure 2. The 6-31G** basis set was used. Empirical dispersion (gd3bj) and solvent interactions (scrf=pcm, acetonitrile) were included in calculations.

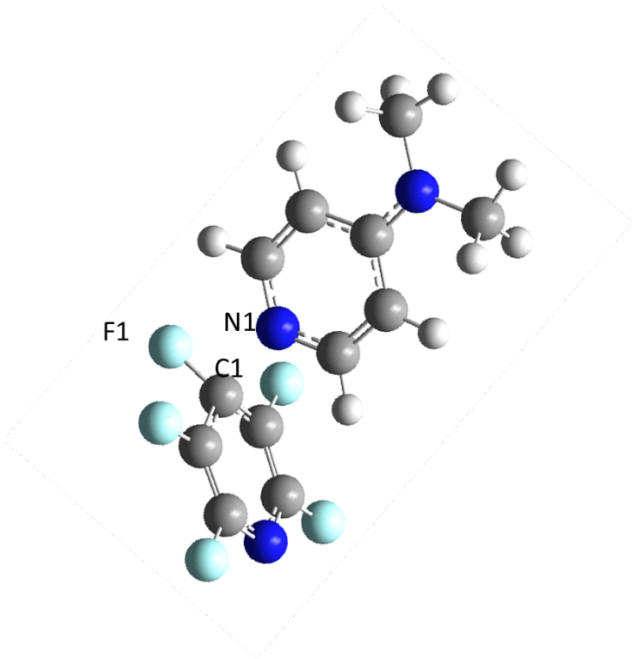

TS-1: N1-C1 = 1.85. C1-F1 = 1.38

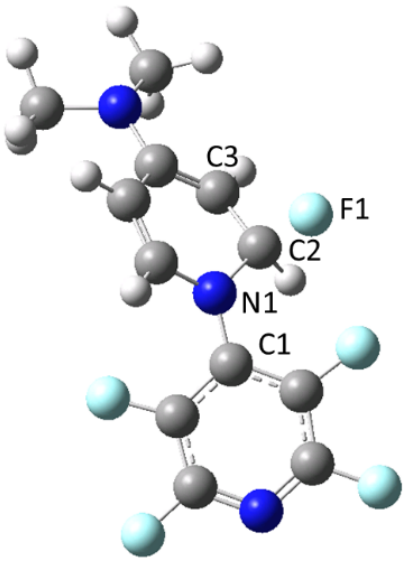

Int-1: N1-C1 = 1.39. C2-F1 = 1.43. C1-N1-C2-C3 dihedral = 146.7

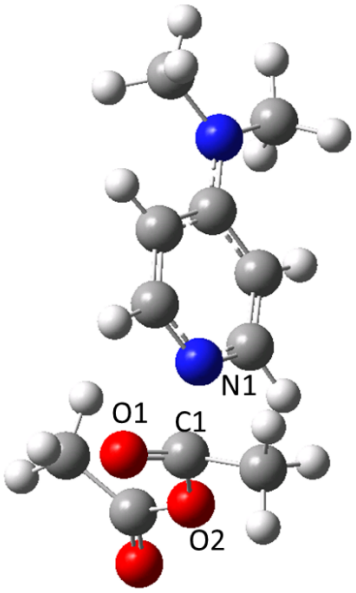

TS-2: N1-C1 = 1.78. C1-O2 = 1.50.

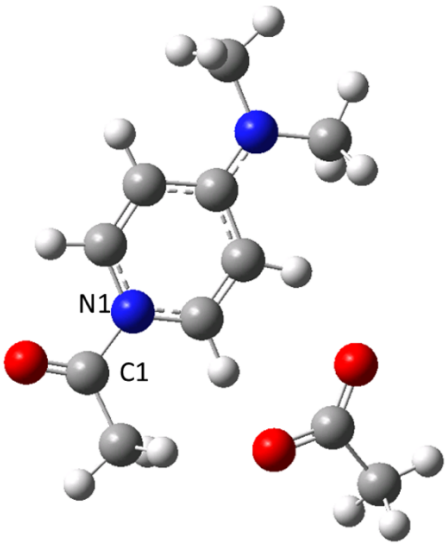

Int-2: N1-C1 = 1.45.

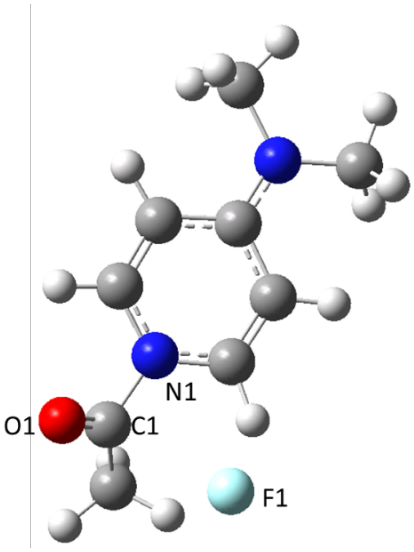

TS-3: C1---F1 = 2.54. C1-N1 = 1.49.
Tetrafluoropyridinium salt omitted for clarity.

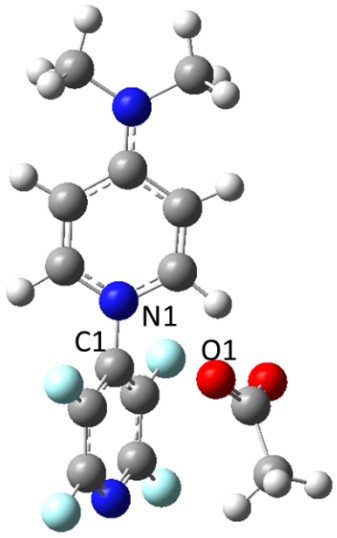

Int-3: C1-N1 = 1.42. C1---O1 = 2.93.

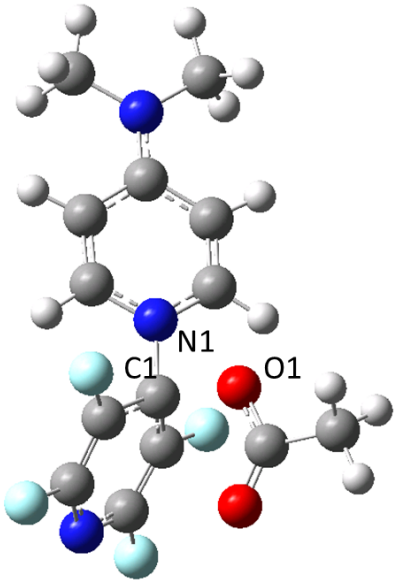

TS-4: N1-C1 = 1.49. C1---O1 = 1.73.

Table S4. Calculated structures of transition states (TS) and intermediates (Int) using B3LYP ((GD3BJ), PCM(acetonitrile)//6-31GG(d,p). Selected bond distances (Å) and angles (°) are reported.

5.2 Mono-Catalysed Pathway

In addition to the dual catalysed reaction pathway presented in Figure 2, the individual mono-catalysed reaction pathways were also considered in Figure S4. For each functional, the overall activation barrier was lower for the dual catalysed pathway than either mono-catalysed pathway. This finding is consistent with kinetic data supporting the conclusion that the turnover-limiting step, and therefore overall reaction pathway, involves two molecules of DMAP.

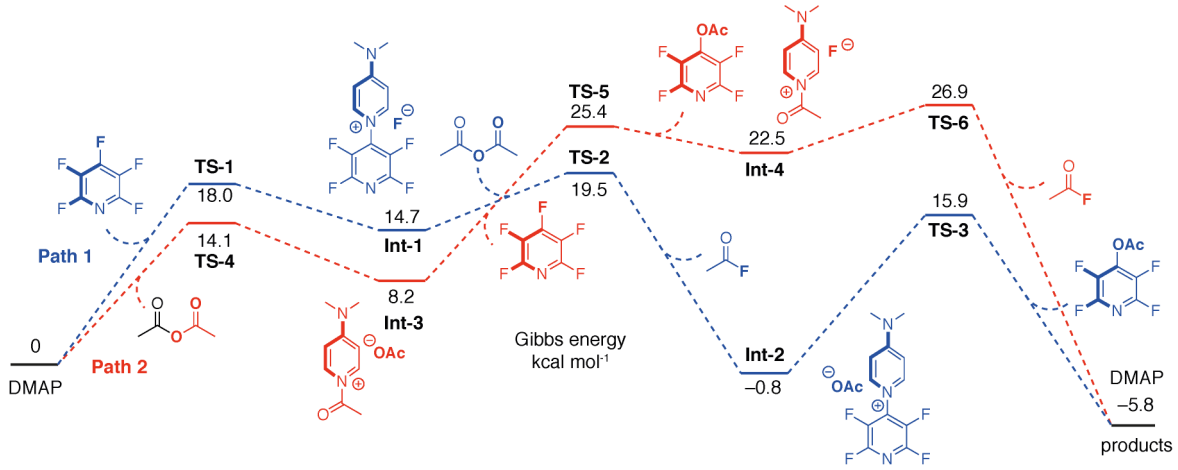

Figure S4. DFT calculated reaction pathways for the mono-catalysed reaction of DMAP, C5F4N and acetic anhydride.

	B3LYP (Kcal mol^{-1})	B3PW91 (Kcal mol^{-1})	WB97X-D (Kcal mol^{-1})
TS-1	18.0	17.9	21.6
Int-1	14.7	14.3	15.8
TS-2	19.1	20.3	21.3
Int-2	-0.8	0.4	2.08
TS-3	15.9	18.3	21.1
TS-4	14.1	13.6	16.5
Int-3	8.2	9.7	11.6
TS-5	25.4	25.3	31.4
Int-4	22.5	22.9	26.0
TS-6	26.9	28.1	31.1
Product	-5.8	-6.3	-6.0

Table S5. Functional testing for the energy profile of the reaction pathways 1 and 2, shown in Figure 2. The 6-31G** basis set was used. Empirical dispersion (gd3bj) and solvent interactions (scrf=pcm, acetonitrile) were included.

In Figure S5, the differences in transition state barriers for key steps of the mono and dual catalysed processes are compared.

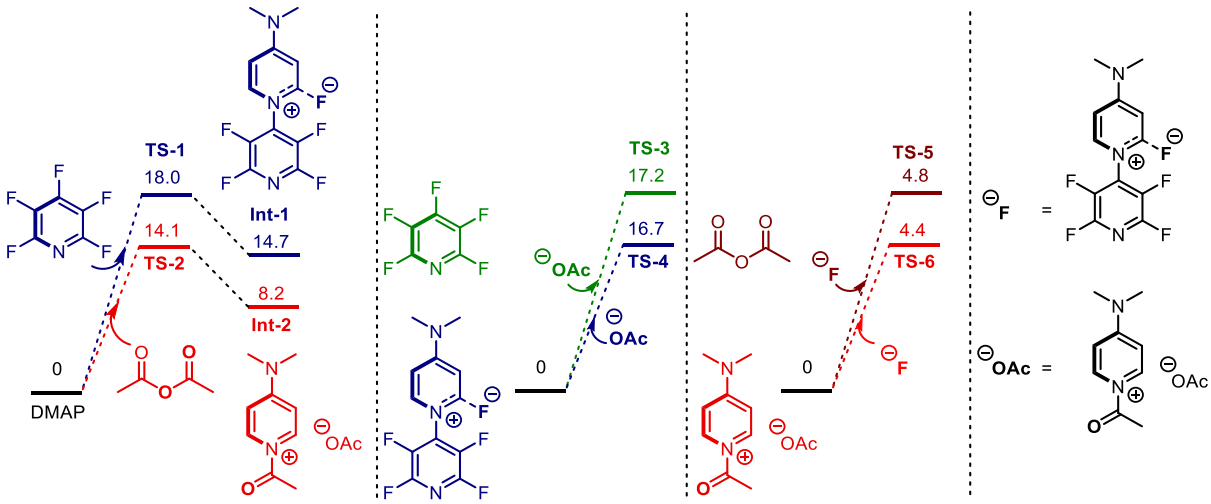

Figure S5. Comparisons of transition state barriers for the mono and dual catalysed reaction pathways. The B3LYP functional and 6-31G** basis set were used. Empirical dispersion (gd3bj) and solvent interactions (scrf=pcm, acetonitrile) were included.

6 Kinetics

Reactions were monitored in situ in a Bruker 500 MHz machine. ^{19}F NMR was conducted with a scan range of 100 to -300 ppm. Scans were performed with a 55 s delay. An FID was collected every 5 minutes. The reactions were conducted at 80 °C to avoid potential bumping of solvent. Reactions were monitored for approximately 16 hours. Conversions were calculated from reagent and product concentrations, based on integration value, relative to an internal standard (1,4-difluorobenzene).

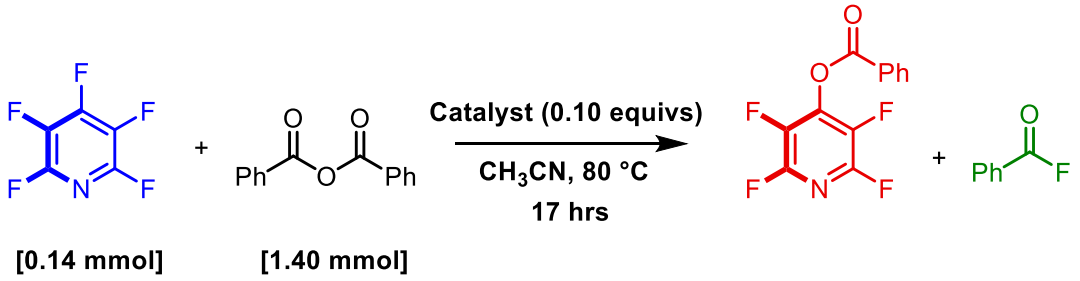

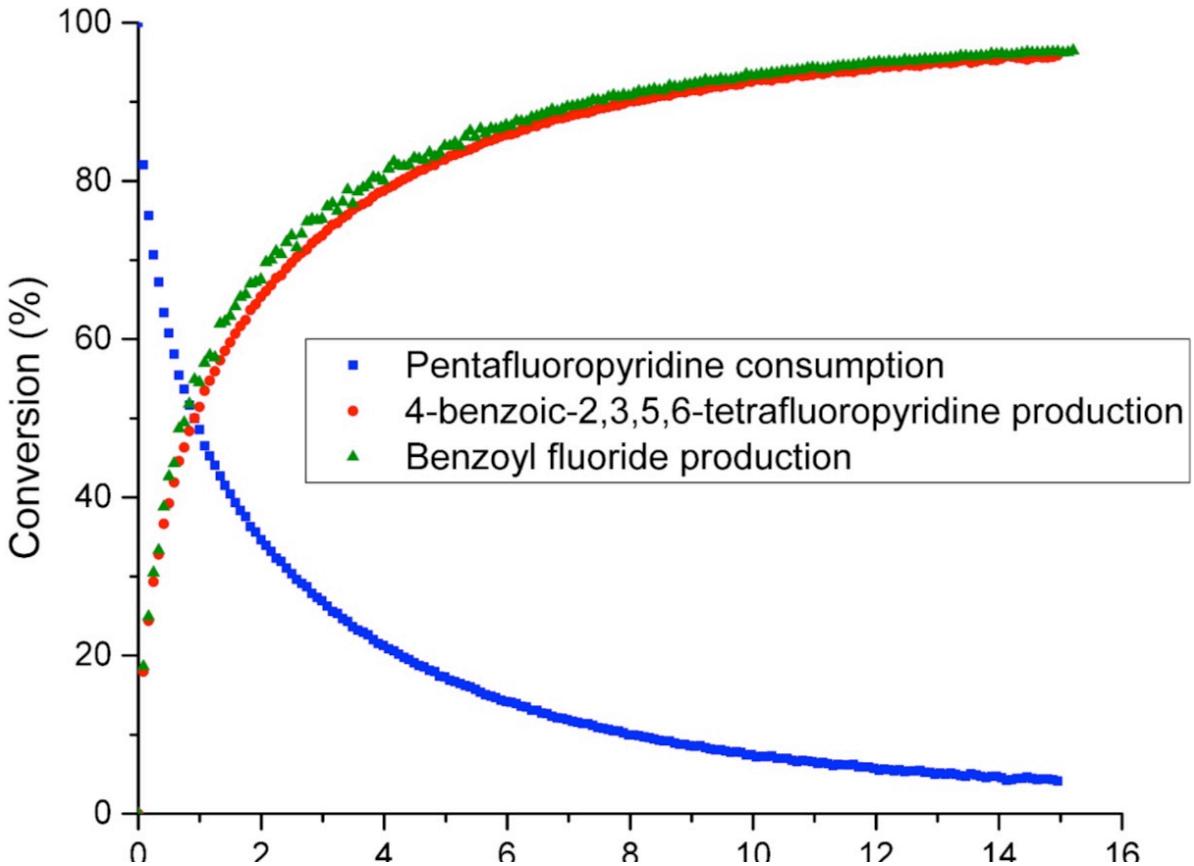

Figure S6. Plot of pentafluoropyridine consumption, 4-benzoic-2,3,5,6-tetrafluoropyridine and benzoyl fluoride production over time.

6.1 Pseudo First Order Reactions.

The rate order in pentafluoropyridine and benzoic anhydride was experimentally verified through pseudo first order reactions. In both cases, when conducting the experiment in an excess of alternate reagent, a plot of the natural logarithm of rate (measured as relative concentration of pentafluoropyridine, [PFP]) against reaction time was shown to be linear, verifying the rate order of both reagents to be one

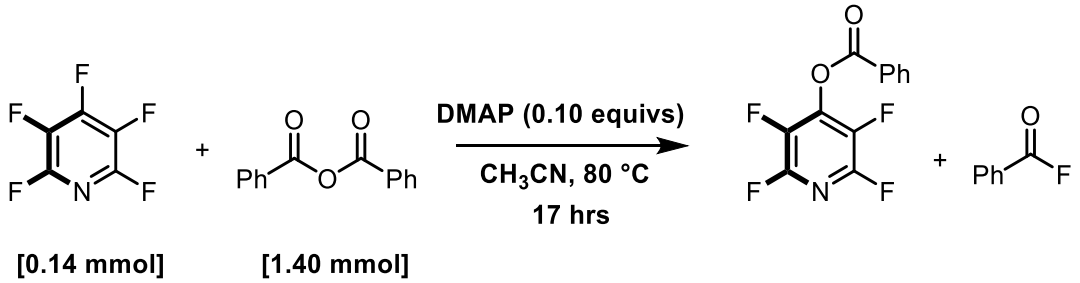

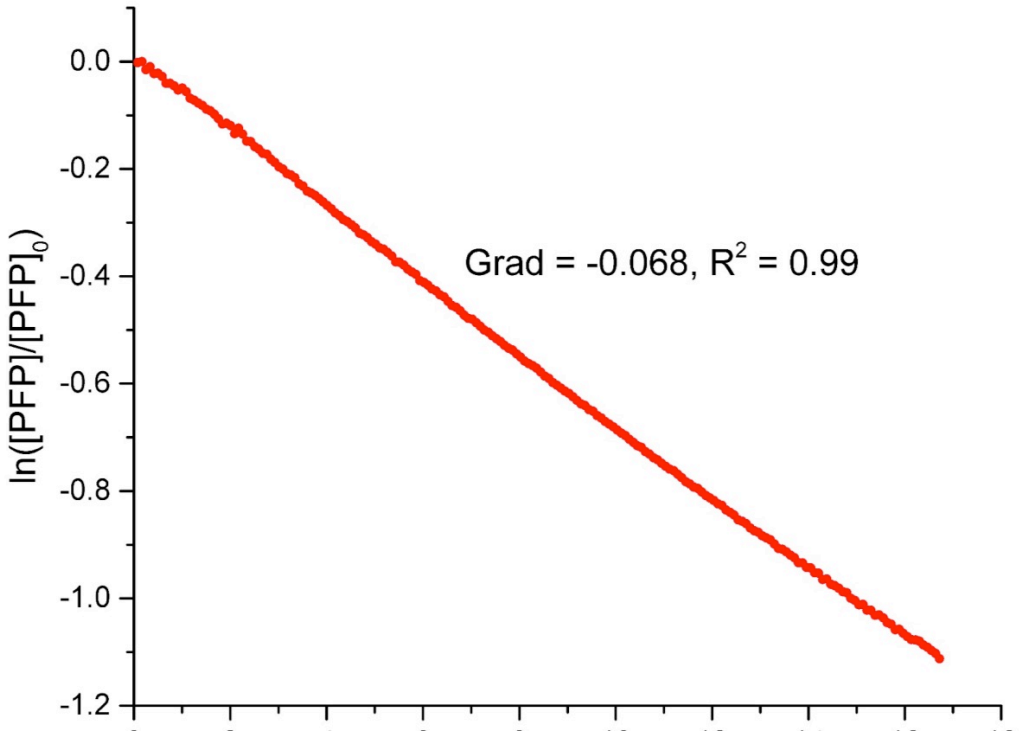

Figure S7. ln plot of consumption of pentafluoropyridine over time, in a 9 equivalent excess of benzoic anhydride.

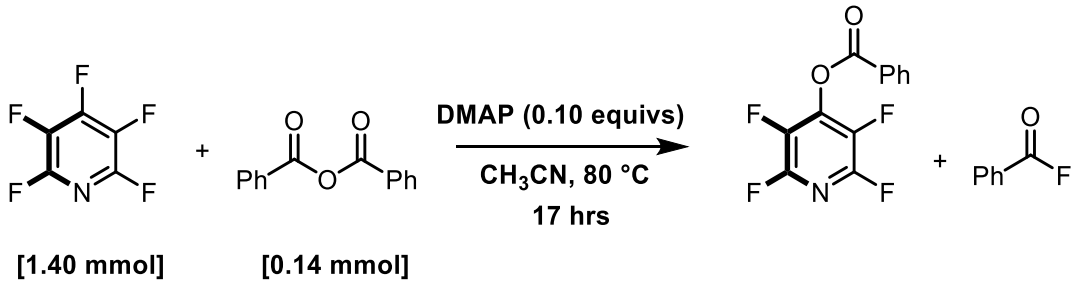

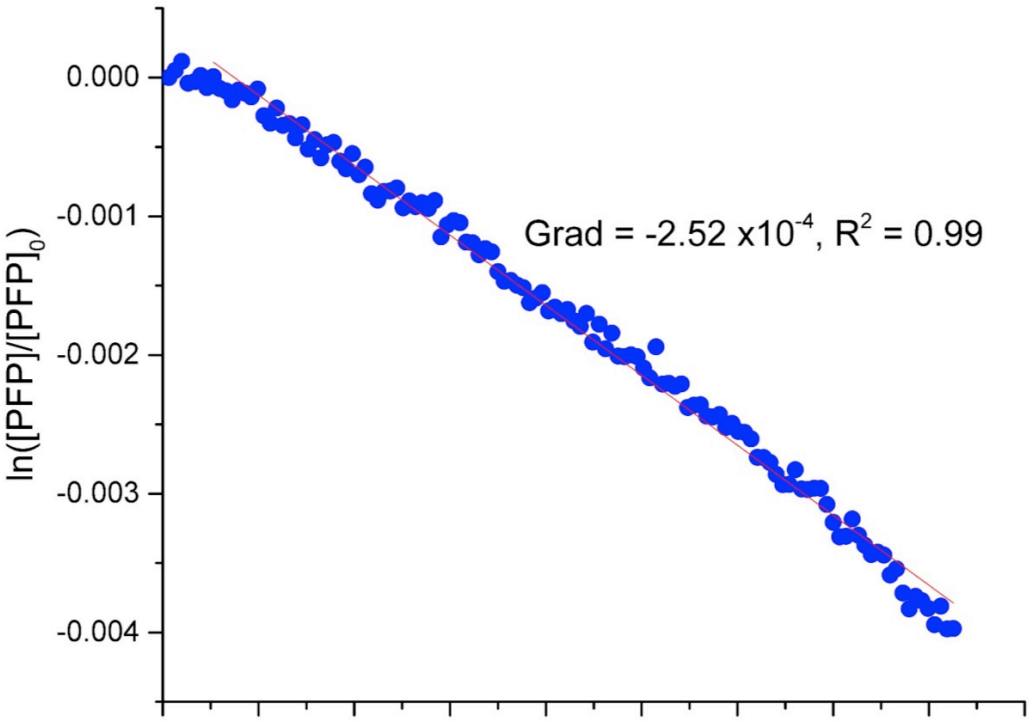

Figure S8. ln plot of consumption of pentafluoropyridine over time, in a 9 equivalent excess of pentafluoropyridine to benzoic anhydride.

A very minor induction period can be observed in this reaction, it does not impact the treatment of this data or affect the overall observation that the rate of consumption of pentafluoropyridine is first order across the reaction timecourse.

6.2 Determining Catalyst Order.

In order to verify the order of catalyst in the reaction, reaction progression was monitored for four catalyst loadings.

A log-log plot of initial rates against total catalyst concentration, shown in Figure S9 suggests a catalyst order of 2. This is consistent with DMAP activation of both PFP and benzoic anhydride in the rate determining step of reaction.

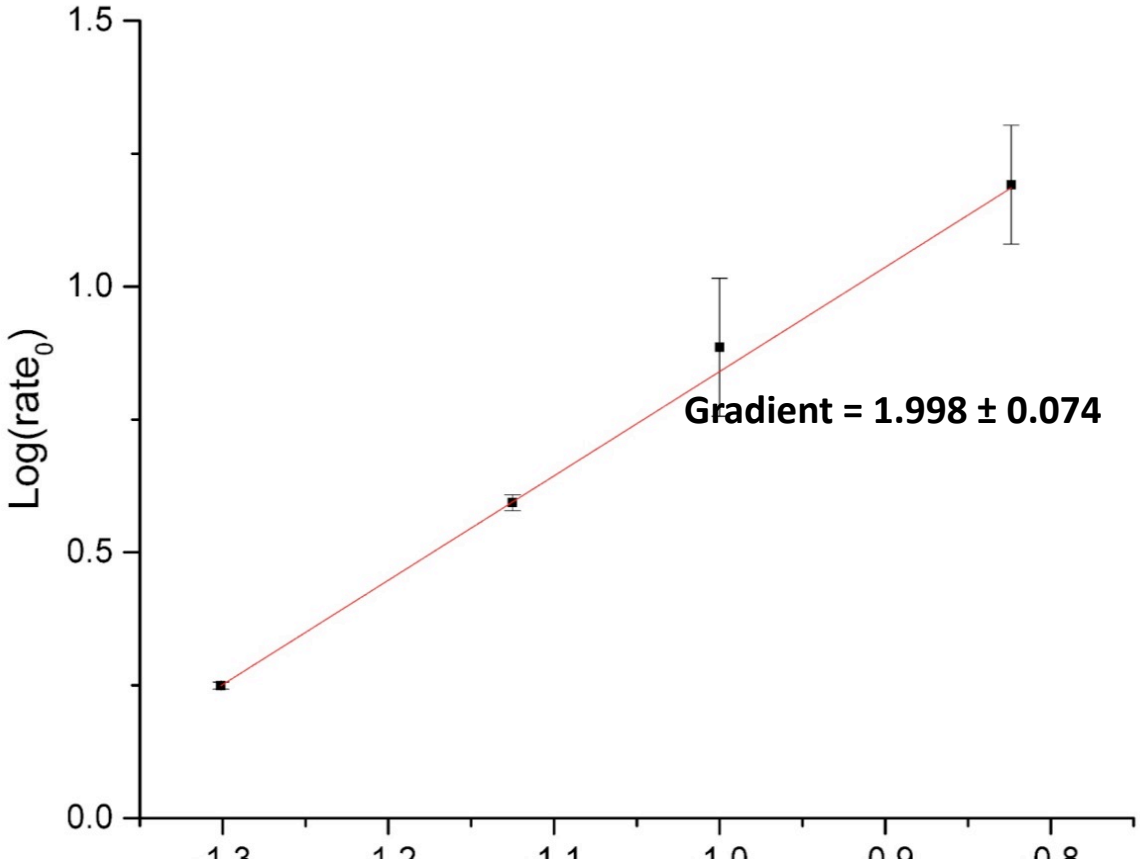

Figure S9. Log-log plot of initial rates ($rate_0$) against total catalyst concentration ($[Cat]_T$) for four catalyst loadings: 0.05, 0.075, 0.10 and 0.15 equivalents. Reactions were set up following general procedure 3i.

In addition to initial rates, graphical analysis was applied to the entire data sets for each catalyst loading. By plotting reaction conversion as concentration of pentafluoropyridine ([PFP]) against reaction time, multiplied by catalyst concentration, to the power of an arbitrary value n ($t[Cat]^n$), the order of catalyst in the reaction can be visually verified as the value of n for which the plots best overlap. As can be seen in Figure S10, this is consistent with a catalyst order of 2, in agreement with the initial rates plot.

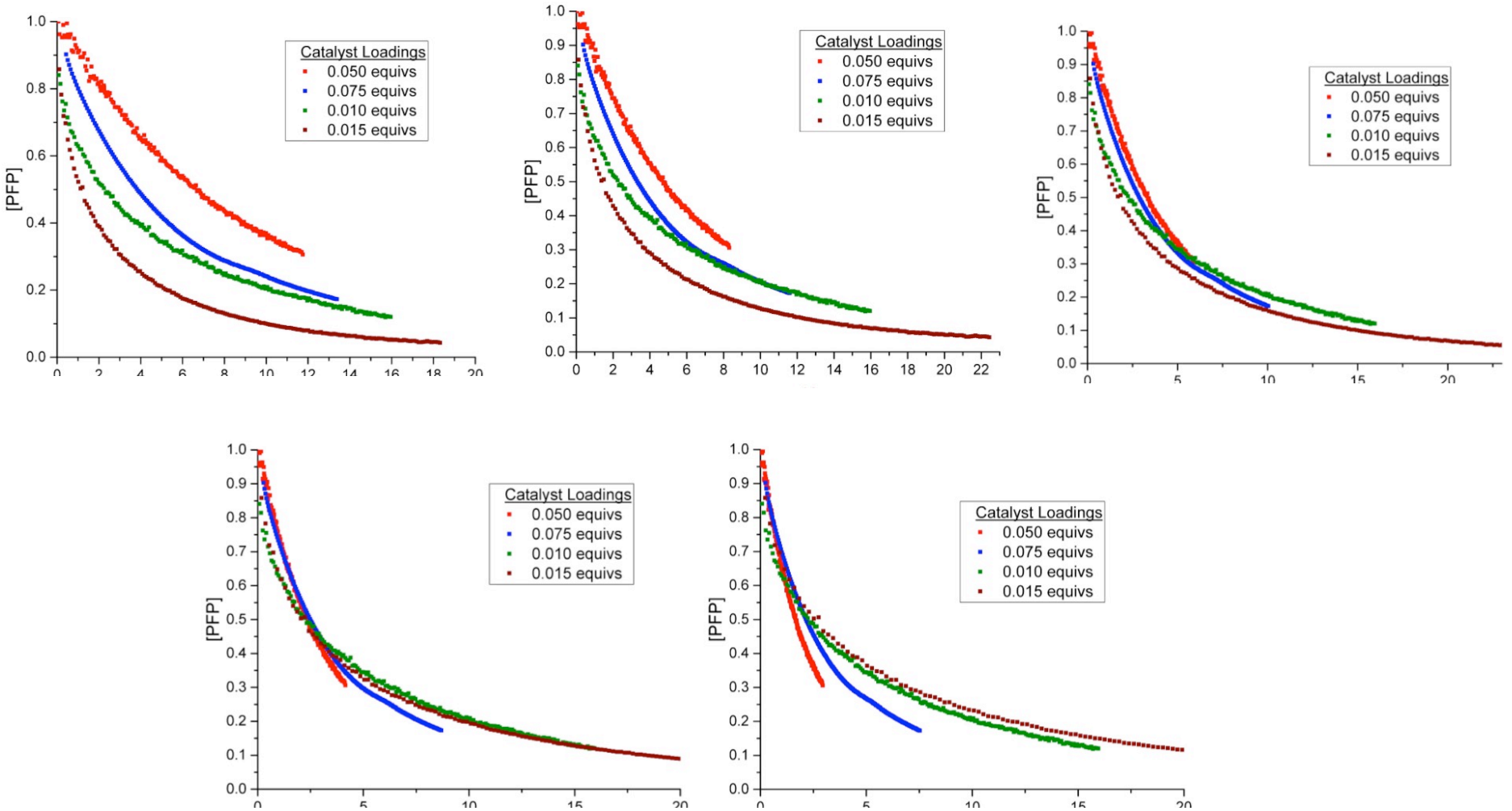

Figure S10. Graphical analysis of the order of catalyst, by plotting [PFP] against t[Cat]^n for each catalyst loading.

7 References

[S1] Senaweera, S.; Weaver, J. D. *Chem. Commun.* **2017**, *53*, 7545.

[S2] Chen, Y.; Qi, H.; Chen, N.; Ren, D.; Xu, J.; Yang, Z. *J. Org. Chem.* **2019**, *84*, 9044.

[S3] Scattolin, T.; Klein, A.; Schoenebeck, F. *Org. Lett.* **2017**, *19*, 1831.

[S4] Morgan, P. J.; Hanson-Heine, M. W. D.; Thomas, H. P.; Saunders, G. C.; Marr, A. C.; Licence, P. *Organometallics* **2020**, *39*, 2116.

[S5] Arisawa, M.; Yamada, T.; Yamaguchi, M. *Tetrahedron Lett.* **2010**, *51*, 6090.

[S6] Cismesia, M. A.; Ryan, S. J.; Bland, D. C.; Sanford, M. S. *J. Org. Chem.* **2017**, *82*, 5020.

[S7] SHELXTL v5.1, Bruker AXS, Madison, WI, 1998.

[S8] SHELX-2013, G.M. Sheldrick, *Acta Cryst.*, 2015, **C71**, 3-8.

7 XYZ Coordinates

TS1.log

SCF (wB97x) = -1126.73767301
E(SCF)+ZPE(0 K)= -1126.526039
H(298 K)= -1126.507080
G(298 K)= -1126.574646
Lowest Frequency = -235.9677cm-1

C	1.330880	-0.375572	-1.366967
C	2.140019	0.452368	-2.109994
C	2.691513	1.696719	-0.337287
C	1.918097	0.947879	0.518834
C	1.114413	-0.118247	0.018534
N	2.832024	1.479050	-1.637177
F	0.992003	-1.224378	0.833135
F	0.646353	-1.396573	-1.935631
F	2.269617	0.196603	-3.426036
F	3.390439	2.726660	0.177466
F	1.819548	1.250355	1.835338
C	-2.868651	0.145466	1.102640
C	-1.563127	-0.279838	0.988124
C	-1.038465	1.469381	-0.439840
C	-2.318987	1.969047	-0.387820
C	-3.300069	1.307863	0.404367
H	-3.545352	-0.420344	1.727342
H	-1.206370	-1.160354	1.506690
H	-0.267129	1.950124	-1.034010
H	-2.555639	2.859531	-0.952549
N	-0.661528	0.369073	0.230224
N	-4.572610	1.760632	0.488165
C	-5.549566	1.055451	1.312921
H	-6.503714	1.575601	1.254337
H	-5.696031	0.027006	0.964702
H	-5.237085	1.027792	2.362576
C	-4.977774	2.954150	-0.249147
H	-6.030015	3.150915	-0.053095
H	-4.399801	3.830594	0.064112
H	-4.848945	2.817872	-1.328627

Int1.log

SCF (wB97x) = -1126.74728233
E(SCF)+ZPE(0 K)= -1126.533570
H(298 K)= -1126.514868
G(298 K)= -1126.579863
Lowest Frequency = 32.0311cm-1

C	0.99446500	2.41700900	-0.09981500
C	3.01003500	3.20896500	-0.68811500
C	2.66062700	4.51985600	-0.39050900
C	0.51723700	3.68216000	0.20944200
N	2.21044000	2.17327400	-0.54310900
C	1.39553800	7.24104000	-0.33702200
C	0.04858400	6.29487600	1.45874500
C	0.35340000	8.28273300	-0.45796200
H	1.76722300	6.91673600	-1.30772600
C	-0.65614300	7.43672200	1.56873900
H	-0.00301000	5.50269800	2.19285600
C	-0.59341000	8.44019300	0.51415000
H	0.44067400	8.95308500	-1.30104600
H	-1.26062000	7.59079400	2.45168600
C	1.36430800	4.79983300	0.07968000
F	4.24822100	2.97063400	-1.13221800
F	0.16844300	1.37466000	0.03427300
F	-0.75787200	3.82589600	0.60421300
F	3.57217200	5.48892600	-0.55383300
N	0.91915200	6.08285000	0.38782400
N	-1.47666200	9.51352900	0.56565800
C	-1.34012000	10.53934100	-0.45635000
H	-1.97692200	11.38665700	-0.19271200
H	-0.30432700	10.88416900	-0.50272400
H	-1.63401900	10.18537700	-1.45752200
C	-2.86571300	9.27170100	0.95327100
H	-3.31701500	10.21397100	1.27450600
H	-3.46006100	8.87015000	0.11810300
H	-2.92708200	8.56754100	1.78132000
F	2.53856900	7.75931600	0.35280100

TS2.log

SCF (wB97x) = -764.058041912
E(SCF)+ZPE(0 K)= -763.794737
H(298 K)= -763.777195
G(298 K)= -763.839816
Lowest Frequency = -111.0737cm-1

C	-4.390718	-1.420517	0.600023
O	-3.767722	-2.260171	1.265112
O	-4.035236	-1.232191	-0.847727
C	-3.731249	-2.238820	-1.695035
O	-3.230647	-1.949519	-2.768301
C	-7.739120	-3.483375	1.174393
C	-6.466352	-2.959157	1.211819
C	-6.936441	-1.469739	-0.503877
C	-8.227787	-1.932355	-0.616703
C	-8.683927	-2.974459	0.240249
H	-7.995579	-4.280081	1.858228
H	-5.696984	-3.316365	1.888588
H	-6.555085	-0.688408	-1.151016
H	-8.873582	-1.494118	-1.364313
N	-6.070418	-1.972632	0.394705
N	-9.947141	-3.456359	0.165669
H	-11.412954	-4.778225	0.839336

H	-9.771337	-5.438181	0.898732
H	-10.297633	-4.239388	2.103621
C	-10.884858	-2.913260	-0.812793
H	-11.843739	-3.415809	-0.700937
H	-11.040582	-1.839750	-0.659887
H	-10.530277	-3.072267	-1.837463
C	-4.065731	-3.658474	-1.308673
H	-3.730585	-3.863441	-0.292202
H	-5.151337	-3.795150	-1.330488
H	-3.606579	-4.333341	-2.030678
C	-4.582397	0.002018	1.110768
H	-5.220890	0.604051	0.462132
H	-5.017226	-0.041144	2.111387
H	-3.599164	0.476985	1.174598

Int2.log

SCF (wB97x) = -764.062234832
E(SCF)+ZPE(0 K)= -763.799199
H(298 K)= -763.779929
G(298 K)= -763.849214
Lowest Frequency = 13.3194cm-1

C	0.481390	1.859104	0.216609
C	1.259542	2.953782	-0.015124
C	0.757531	4.269281	0.210601
C	-0.593116	4.364685	0.681908
C	-1.328965	3.239975	0.890493
H	0.891168	0.858854	0.011293
H	2.252931	2.733195	-0.390125
H	-1.056235	5.320734	0.879157
H	-2.351610	3.256762	1.239505
N	-0.809958	1.988360	0.667432
N	1.506072	5.357273	-0.009934
C	2.881396	5.214406	-0.496932
H	2.899681	4.708935	-1.466720
H	3.319171	6.203483	-0.609995
H	3.486324	4.641541	0.211648
C	0.965259	6.698422	0.225601
H	0.677246	6.824661	1.273468
H	1.730770	7.433196	-0.012548
H	0.094545	6.885859	-0.409866
C	-1.665067	0.837953	0.906882
O	-2.814921	1.031464	1.231370
C	2.936411	-0.187518	-1.125660
O	3.374677	0.992109	-1.090004
O	1.837814	-0.610003	-0.647685
C	-1.034176	-0.513632	0.753724
H	-0.539226	-0.640833	-0.211637
H	-0.259580	-0.650767	1.514828
H	-1.814727	-1.260596	0.888669
C	3.813573	-1.254243	-1.810458
H	4.094860	-2.025782	-1.084742
H	3.244571	-1.755830	-2.600865
H	4.720084	-0.819784	-2.238241

TS3.log

SCF (wB97x) = -635.375146067
E(SCF)+ZPE(0 K)= -635.162622
H(298 K)= -635.148269
G(298 K)= -635.203191
Lowest Frequency = -145.7197cm-1

C	0.647137	1.808953	0.686427
C	1.372362	2.928061	0.373685
C	0.759484	4.214865	0.320045
C	-0.628092	4.273223	0.654989
C	-1.305920	3.127796	0.963451
H	2.432574	2.812353	0.197960
H	-1.168366	5.208486	0.669543
H	-2.356634	3.122980	1.221597
N	-0.689071	1.914824	0.949204
N	1.451587	5.320527	-0.011627
C	2.874360	5.228802	-0.340088
H	3.038586	4.540995	-1.175077
H	3.233270	6.213662	-0.631106
H	3.459008	4.886499	0.520351
C	0.799604	6.630398	-0.013844
H	0.433984	6.892139	0.984473
H	1.521294	7.383051	-0.323872
H	-0.040424	6.649320	-0.715183
C	-1.517992	0.709526	1.224278
O	-2.312805	0.786665	2.129287
C	-1.422937	-0.371236	0.192154
H	-0.470835	-0.867507	0.415523
H	-2.262749	-1.054870	0.322056
H	-1.424860	0.051962	-0.815899
H	1.014891	0.785597	0.923024
F	0.632632	-0.451807	1.914774

Int3.log

SCF (wB97x) = -1255.41990278
E(SCF)+ZPE(0 K)= -1255.157410
H(298 K)= -1255.133784
G(298 K)= -1255.211452
Lowest Frequency = 26.9732cm-1

C	1.382468	2.738610	-1.409951
C	3.194791	3.682672	-0.440745
C	2.499413	4.840695	-0.118973
C	0.577647	3.838748	-1.130478
N	2.651129	2.663680	-1.073888
C	-0.203038	6.751256	-1.250648

C	0.305506	6.582804	1.068535
C	-0.923568	7.889316	-1.022593
H	-0.021230	6.312117	-2.238862
C	-0.395148	7.718685	1.341673
H	0.807672	6.012422	1.837741
C	-1.056120	8.429842	0.291224
H	-1.381228	8.371882	-1.874036
H	-0.437648	8.055014	2.366868
C	1.153281	4.920727	-0.470258
F	4.488158	3.595199	-0.119611
F	0.846927	1.698770	-2.053071
F	-0.708511	3.854365	-1.480592
F	3.103766	5.860509	0.493598
N	0.398166	6.096031	-0.206654
N	-1.760868	9.545301	0.533577
C	-2.415162	10.258836	-0.565572
H	-2.920643	11.134508	-0.165043
H	-1.682095	10.590310	-1.307188
H	-3.157797	9.623381	-1.057587
C	-1.880684	10.067689	1.896956
H	-2.506206	10.957071	1.878464
H	-2.347174	9.331145	2.558123
H	-0.900780	10.340872	2.300529
C	2.061418	5.644888	-3.427862
O	2.464540	6.481631	-2.576763
O	0.852751	5.325566	-3.650891
C	3.130062	4.878323	-4.229278
H	3.404406	3.971988	-3.675296
H	2.749904	4.565341	-5.205357
H	4.036961	5.475785	-4.354947
H	-0.402785	8.120354	2.214026
C	1.549936	5.324460	-0.819812
F	3.874923	3.435016	1.270412
F	0.437485	1.864980	-1.251895
F	-0.286275	4.365579	-2.012488
F	3.317348	6.006423	0.641995
N	0.720562	6.526845	-0.501202
N	-1.843435	9.641586	0.491403
C	-2.568472	10.362911	-0.555708
H	-3.164608	11.147189	-0.094690
H	-1.874868	10.826727	-1.264023
H	-3.239865	9.692988	-1.102260
C	-2.031129	10.026464	1.891160
H	-2.721416	10.865847	1.935941
H	-2.451898	9.200441	2.473254
H	-1.083170	10.333468	2.343761
C	3.136548	5.328594	-2.886646
O	3.433514	4.163900	-2.652173
O	2.289301	6.069041	-2.189798
C	3.723471	6.108357	-4.052171
H	2.925270	6.412297	-4.736223
H	4.207054	7.019875	-3.689379
H	4.447847	5.491450	-4.585309

TS4.log

SCF (wB97x) = -1255.39350023
E(SCF)+ZPE(0 K)= -1255.131857
H(298 K)= -1255.109076
G(298 K)= -1255.184298
Lowest Frequency = -225.3298cm-1

C	1.161848	2.912497	-0.806459
C	2.842004	3.682481	0.438900
C	2.554470	4.991152	0.146256
C	0.778373	4.170527	-1.186540
N	2.177796	2.625743	-0.003390
C	0.037880	7.192646	-1.474164
C	0.524946	6.871164	0.800879
C	-0.816249	8.218794	-1.178911
H	0.223290	6.866670	-2.484033
C	-0.303640	7.895560	1.162228
H	1.062923	6.287650	1.533541
C	-1.020528	8.629039	0.170906
H	-1.326158	8.703248	-1.998642